METRANS

Task Order No.: TO 018.2 (Shailesh Chandra) Contract No.: 65A0533

Evaluating economic mobility and resilience of multimodal freight operations in a connected vehicle environment

Final Report

Shailesh Chandra, Ph.D.
Jose Jimenez
Annie Nguyen
Liliana Iniguez

Department of Civil Engineering and Construction Engineering Management
California State University, Long Beach

Submission Date: February 28, 2018

Contents

Executive Summary

Connected Vehicle Technology (CVT) has the potential to become very relevant and crucial for multimodal transportation, which involves a synchronized operation of two or more modes of freight (such as trucks, rail, air cargo and ports) responsible for transfer of essential goods and commodities on a large scale. However, very little is known about the influence of reliability of CVT network on the freight industry. Therefore, this research will aim to understand the implications of CVT implementation for multimodal freight operations in determining efficient routes for mobility and resilience with connected vehicles' network reliability. The influence of CVT using vehicle-to-vehicle (V2V) and vehicle-to-infrastructure (V2I) communications on routing of the freight vehicles in the multimodal operations becomes critical for commercial trucks, which, unlike freight rail, have some flexibility in detouring and deviating in order to access other links and nodes of the highway network to complete a trip. Thus, for trucks, reliability of communication network of CVT for proper route guidance becomes paramount. A perfectly reliable communication network would be a network in which all freight vehicles constituting the multimodal freight system exhibit CVT and communicate with each other during transport operations.

The theoretical indicators for mobility and resilience developed in this research are time-sensitive and vary between 0 and 1. This assists in easy interpretation in the multimodal context. Thus, an indicator value of 0 denotes poor or low mobility/resilience and a value of 1 denotes high mobility/resilience of a route/path being examined. The tonnage values for each of the links constituting the 11 to 15-mile length are obtained from the year 2012 Freight Analysis Framework (FAF) data- which help in estimating parameter values used in the indicators. The parameter value is found to be in the range of 5 to 12 for the routes of I-405, I-5, I-10 and I-710. These interstates connect one or more intermodal terminals and ports in the Southern California Region. It is also noted that for the length of the segments selected for the routes, I-10 appears to the be worst in terms of the mobility indicator, while ranks better than all the routes in terms of the resilience indicator. I-710 appears to be having much better mobility as compared to rest of the routes. This could be due to high truck volumes experience on the interstate resulting in large total tonnage value. Thus, these values of mobility and indicator obtained here can be used in future as elements

to design Connected Vehicle Technology or Intelligent Transportation System where rerouting of vehicles will be necessary to produce an efficient freight network.

In this research, a probabilistic model for reliability of the communication network is developed and it relates it to travel time changes for mobility as well as (during disruptions) for resilience. The modeling for network reliability is being carried out as a percolation process which is known to mimic failures in links/nodes quite precisely in a network of any given size. Findings in this research indicate that decreasing the value of micro-level reliability, the macro-level reliability will tend to decrease as well. This can be further corroborated with the fact that a low micro-level reliability among individual vehicles of a cluster on an average will lead to low macro-level reliability of the group of clusters.

Further, it is observed that the ratio of theoretical number of vehicles with sensors to total number of vehicles on highway is almost 1 when the optimum radius of transmission range is greater than 1500 feet for traffic densities lower than 9 veh/mile (under sparse traffic conditions). This optimum radius for transmission range is higher than 55 feet for traffic densities lower than 100 veh/mile with dense traffic conditions. Irrespective of the density of the freight vehicles around an intermodal terminal, port or airport (i.e. congested or uncongested highway with trucks), the expression for the average distance to the closest freight truck does not change. As the length of the highway segment increases, there is linear increase in the average size of connected *k*-component (i.e. *k* trucks). However, there is exponential increase in the average size of the connected *k*-component (trucks) with increase in density of vehicles and/or with increase in sensor transmissions radius. This information is useful in determination of optimum radius of sensor radius when freight vehicles are moving in a platoon.

Cost estimation of routes on I-405, I-5, I-10 and I-710 show that there are savings in fuel costs per hour for the ‘with CVT’ as compared to the ‘without CVT’ case. In addition, there is significant increase in total tonnage transported under ‘with CVT’ case as compared to the ‘without CVT’ case for all the four routes analyzed.

Introduction and Background

Commercial trucks, freight rails, seaports and airport, which are part of multimodal freight transportation, are indispensable to a nation's economic competitiveness. The recent enactment of Fixing America's Surface Transportation Act (FAST Act) into law in December 2015 recognizes the importance of investment in transportation, particularly for sustained economic growth of freight industry in the United States. The Fast Act will address conditions and performance of multimodal freight transportation system for mobility.

The FAST Act includes provisions for establishing a National Multimodal Freight Policy which will "address the conditions and performance of the multimodal freight system, identify strategies and best practices to improve intermodal connectivity and performance of the national freight system" [1]. These provisions expressed in the FAST Act regarding multimodal freight are concurrent with several on-going research programs that the United States Department of Transportation (USDOT) supports which will improve safety, mobility and environment through connected vehicle technology (CVT) in the area of Intelligent Transportation Systems (ITS) for freight [2].

Concurrent to the impetus received through the FAST Act is the United States Department of Transportation's (USDOT's) on-going programs. The ITS Strategic Plan 2015-2019 of USDOT prioritizes design, testing, and planning for deployment of connected vehicles across the nation. Realizing connected vehicle implementation and advancing automation in the freight industry will be crucial in the success of ITS Strategic Plan, since freight contributes by connecting various industry sectors to the international gateways of the country through a system of multimodal freight network. Thus, within the context of multimodal freight, connected vehicles will command special significance in boosting economic mobility and resilience of freight operations.

The USDOT's keen interest in adoption of automation-related technologies reflected in its preamble of ITS Strategic Plan, has spurred several private freight manufacturing companies, such as the Volvo Group, to roll out their next generation fleet of freight vehicles, especially commercial trucks, to be integrated with ITS and connected vehicle technology (CVT) features.

The current transformation that the freight industry is undergoing with regard to integration of CVT into its next generation fleet of vehicles, it is expected that all modes constituting a multimodal freight transportation system will "talk to each other" and will adapt to changes in their surrounding traffic conditions leading to efficient freight operations. While safety, mobility

and environmental benefits are clearly accrued and anticipated from ubiquitous CVT exhibited by a freight vehicle at the micro level, the role of the technology in mobility and resilience building of multimodal freight operations is currently unknown or at least needs an initial probe/investigation at the macro level for freight planning purposes.

CVT has the potential to become very relevant and crucial for multimodal transportation, which involves a synchronized operation of two or more modes of freight (such as trucks, rail, air cargo and ports) responsible for transfer of essential goods and commodities on a large scale. However, very little is known about the influence of reliability of CVT network on the freight industry. Therefore, this research aims to understand the implications of CVT implementation for multimodal freight operations consisting of ports, intermodal terminals and airports.

In order to make this research useful for a larger audience consisting of engineers, planners and practitioners associated with the multimodal freight industry, data related to freight operations from the Southern California region is being used for demonstration purposes.

Several states in the nation have initiated and/or have adopted pilot programs to further the efforts of the USDOT in CVT research. For example, the proposal, called "One California," which embodies the principles identified in the California Transportation Plan 2040 is already looking at CVT application-centric approach, both technically and scientifically, in creating a sustainable and interconnected transportation system in California [3].

Private automobile companies, such as the Volvo Group, are also showing keen interest in leveraging this government-led initiatives and programs to modernize their next generation freight fleet with connected vehicle technologies [4]. This will enable freight trucks to communicate with the infrastructure as well as with other vehicles present in the transportation network through Intelligent Transportation Systems (ITS) applications.

Therefore, with the high level of patronage that the CVT is receiving both from the public and private stakeholders in freight, it is expected that in coming years a large number of commercial trucks and other freight vehicles within a multimodal framework will exhibit increased vehicle-to-vehicle (V2V) and vehicle-to-infrastructure (V2I) communication capabilities.

Connected vehicle initiatives for freight industry from the USDOT is relatively new. Out of the three recently announced pilot programs by the USDOT for next generation connected vehicle technologies implementation, Wyoming is the only state which is focusing on evaluating efficiency and safety of freight movement on I-80 corridor by using V2V and V2I communication

technologies [5]. Corridors in other states might soon become testbeds for such pilot program implementations of CVT. This will naturally augment the National Multimodal Freight Policy set up by the FAST Act to address performance of multimodal freight operations. As CVT begins to get integrated with the freight movements for better operations, the reliability of the CVT communication network itself would become very crucial.

With high reliability exhibited by CVT-induced communication network, freight vehicles from various modes (such as trucks, rail, air cargo and ports) would be assisted dynamically in route guidance. The guidance will involve avoiding congested and/or disrupted links and nodes on a physical multimodal network system consisting of highways, rail tracks, sea routes etc. leading to an increased mobility and resilience of the multimodal freight operations. Currently, there are no literatures or studies that add to our knowledge or understanding of easily computing and locating high impact freight routes or areas where implementation of connected vehicle technologies would benefit economic mobility and resilience of multimodal freight operations. This is what this research will explore and evaluate both at the theoretical level treating both mobility and resilience of multimodal freight network as surrogates to multimodal freight performance. Reliability of V2V and V2I communication network exhibited by individual freight modes on a macro level will serve as input to assessing economic components of mobility and resilience of the multimodal freight operations.

CVT in this research is defined as the sensor transmission-based interaction of information among multimodal transportation entities (such as freight vehicles, intermodal terminals etc.) on mobility, safety and location of vehicles in an area of analysis.

Literature Review

Multimodal Transportation has been defined as the "movement in which two or more different transportation modes are linked end-to-end in order to move freight and/or people from point of origin to point of destination" ([6], [7]). By using either multimodal shipping or intermodal shipping various modes of transportation will be able to reduce some of the negative factors of dealing with only one mode of transportation. Both intermodal and multimodal shipping have the potential to optimize travel times, reducing inventory cost, reducing freight transportation cost, and overall improving freight operations ([8], [9], [10]). The recent enactment of FAST Act into

law in December 2015 recognizes the importance of investment in transportation, particularly for sustained economic growth of freight industry in the United States [11].

Furthermore, through the FAST Act a National Multimodal Freight Policy that includes national goals to guide decision-making will also be established. The National Multimodal Freight Policy that will address the conditions and performance of the multimodal freight system, while identifying strategies and best practices to improve intermodal connectivity and performance of the national freight system [12]. This will be accomplished in hopes of alleviating the impacts of freight movement on communities and thus, with the potential to improve mobility and resilience of multimodal freight transportation.

Travel time is vital in freight operations for a sustained growth of business [13]. This is due several modes of transportations being used to transport containers from one location to another [14]. For a transport system to function properly and even optimally, each of its mode must operate in tandem under certain predicted travel time ranges to cause minimal delay to any other part of the system and be able arrive at their destinations in time. The importance of punctuality in arriving to the terminals is due to these terminals being either the point of origin, termination, interchange, or of transfer. Therefore, delayed arrivals to these terminals cause late pick- ups, delayed deliveries, or delays for the other modes of transportation waiting for the freight, which in turn results in high transportation costs ([15], [16]).

Measures of Mobility

Numerous literatures define mobility as measure for performance in the context of congestion for various freight modes. A compilation of these measures has been presented in Table 1:

Table 1: Compilation of mobility/congestion measures in literatures

Definition/Explanation	**Source (s)**
Mobility Scorecard (Yearly delay per auto commuter (hours); Travel Time Index; Planning Time Index (Freeway only) ; “Wasted" fuel per auto commuter (gallons); Congestion cost per auto commuter (2014 $); Travel delay (billion hours); “Wasted” fuel (billion gallons); Truck congestion cost (billions of 2014 dollars); Congestion cost (billions of 2014 dollars)	2015 Urban Mobility Scorecard (2015) [17]
The shipment of cargo and the movement of people involving more than one mode of transportation during a single, seamless journey	Bontekoning (2004) [18]; Jones (2000) [19]

Movement in which two or more different transportation modes are linked end-to-end in order to move freight and/or people from point to origin to point of destination	Southworth (2000) [20]
Transport of goods in containers that can be moved on land by rail or truck and on water by ship or barge. In addition, intermodal freight usually is understood to include bulk commodity shipments that involve transfer and air freight (truck–air)	TRB (1998) [21]
The movement of goods in one and the same loading unit or vehicle, which uses successively several modes of transport without handling the goods themselves in changing modes (European Commission, 1997)	Tsamboulas (2000) [22]
The movement of goods in one and the same loading unit or vehicle, which uses successively several modes of transport without handling the goods themselves in changing modes (European Conference of Ministers of Transport, 1993)	Van Duin (1998) [23]
Personal mobility is interpreted to mean the ability of individuals to move from place to place: this depends principally upon the availability of different modes of transportation, including walking (see Hillman ef al. 1973, 1976). When defined in this sense, mobility is conceptually distinct from actual travel	Morris (1979) [24]
Congestion analysis Congestion detection is performed by calculating the Mahalanobis distance between real time data and the corresponding time slot in the traffic model. If the distance calculated is greater than a specified threshold d_high, it signals a certain incident causing congestion in the area of analysis. Mahalanobis distance between vector $\vec{X}$ (real time vehicle data) from a group of values with mean $\vec{\mu}$ (calculated from historical data) is calculated using expression (1) below: $d(\vec{X},\vec{\mu}) = \sqrt{(\vec{X}-\vec{\mu})S^{-1}(\vec{X}-\vec{\mu})}$ $d(\vec{X},\vec{\mu}) \sim \chi^2_{n-1}$	Bhattacharya (2014) [25]
Intermodality According to Mahoney (1986), ‘‘Intermodality’’ is the movement of freight via two or more dissimilar modes of transportation. Hayuth (1987) defines it as the movement of cargo from shipper to consignee by at least two different modes of transport under a single rate, through-billing, and through liability. In general, research in the area of intermodal transport systems not only assists in developing effective transport networks, but also contributes to reducing negative impact on environment and energy consumption. In developing countries such a system will drastically improve the utilization of transport resources and services, leading to better scheduling and delivery with lower logistics costs and higher levels of efficiency.	Bhattacharya (2014) [24]; Hayuth (1987) [27]; Mahoney (1986) [28]

Congestion Index $\overline{t_s} = \overline{t}_{b,S} + \overline{t}_{w,S}$ $= \frac{1}{\mu} + \frac{a^S}{\mu(S-1)!\,(S-a)^2}\,[\sum_{n=0}^{S-1}\frac{a^n}{n!} + \frac{a^S}{(S-1)!\,(S-a)}]^{-1}$ $\lambda = avg\ arrival\ rate\ of\ ship\ \left(\frac{vessel}{day}\right)$ $\mu = avg\ service\ rate\left(\frac{vessels}{day}\right)$ $S = number\ of\ berths$ $\overline{t}_{b,S} = avg\ time\ ships\ are\ present$ $with\ S\ berths\ \left(\frac{days}{vessel}\right)$ $\overline{t}_s = avg\ time\ ship\ are\ served\ at$ $wharf\ with\ S\ berths(= \mu^{-1},\ \left(\frac{days}{vessel}\right)$ $\overline{t}_{wS} = average\ waiting\ time\ with$ $S\ berths\ \left(\frac{days}{vessel}\right)$ $a = traffic\ intensity\ \left(\frac{\lambda}{\mu}\right)$	M. Noritake (1985) [29]
Congestion Index $RCI = \frac{[(Fwy_{DVMT} \times Fwy_{DVM}) + (Art_{DVMT} \times Art_{DVM})]}{13{,}000 \times Fwy_{DMV} + 5{,}000 \times Art_{DVM}}$ RCI: $Roadway\ Congestion\ Index$ Fwy: $Freeway$ ($assumed\ capacity$ 13,000 $DVMT$) Art: $arterial\ roadway$ ($assumed\ capacity$ 5,000 $DVMT$) $DVMT$: $Daily\ Vehicle\ Miles\ per\ Lane - Mile$ DVM: $Daily\ Vehicle\ Miles$	Hamad (2002) [30]; Schrank (1990) [31]
Congestion Index $Congestion\ Index$ $= \frac{Travel\ Rate_{Actual\ for\ Section\ (\frac{min}{mi})} + Travel\ Rate_{Acceptable\ (\frac{min}{mi})}}{Travel\ Rate_{Acceptable\ (\frac{min}{mi})}}$	Taylor (1992) [32]; D'Este (1999) [33]

Measures of Resilience

Resilience (and also vulnerability) have been used quite widely in transportation literatures ([34], [35], [36], [37]). However, in most of the literatures resilience strategies and principles are not very well tied with multimodal freight performance metrics. As a recent report by Hughes and Healy (2014) [38] points out, this is mainly because resilience principles differ in their definition and application. Added to the complexity are the uncertainties in types, magnitudes and frequencies of causes and failure modes for freight operations. The National Infrastructure Advisory Council (NIAC) developed a set of recommendations for establishing critical infrastructure resilience goals under four broad categories – of robustness, resourcefulness, rapidity and adaptability (NIAC 2010) [39].

Robustness is the ability to absorb shocks with continuous operations, resourcefulness is the management of disruption as it unfolds rapidity deals with the ability to revert to normal conditions as quickly as possible and adaptability allows absorbing new lessons learned after a disaster. Although the four principles together serve as good performance criteria for resiliency for any general incident response planning purpose, not sufficiently though for freight. Critical to a carrier's and shipper's needs are also the redundancy aspect of freight operations that should be appropriately incorporated within the selected set of resiliency principles.

The freight transportation network in California is large and complex. However, with such a vast and complicated network issues concern timing and unforeseen accidents can cause delays and sometimes result in segments of a network needing to wait for the other parts of the network to improve due to being unable to restart operations after incidents occur. Therefore, a possible method for optimizing the freight transportation network is integrating CVT in multimodal freight operations. CVT might be used to improve the resilience of a multimodal transportation network. By using CVT, it would be possible to become informed of any issue that can result in delays and could even guide users in a direction that can help minimize the effect of any unforeseen event may have had on the system [40]. Furthermore, seeing as how the majority of surface freight transport occurs on roads it is vital that the technology used focuses on trying to improve that section of freight operation. This can be accomplish improving the communication that occurs between other vehicles to avoid situations that could worsen traffic condition due to the presence

of freight trucks and in the same time cause delays throughout the freight transportation network. Additionally, improving the communication occurring between not only freight trucks but also involving the other mode of transportation involved allow decision-making to also become optimized due to the ability to now take into account all delays in every mode involved in the process and thereby plan for situations in which operation may be affected in order to minimize its effect on the system.

While a mobility indicator represents the level of congestion on the link/node, a resilience indicator will signify ability of the link/node to absorb shocks or disruptions and continue to assist in multimodal freight operations. Several literature address network resilience in conjunction with network vulnerability [41]. For example, Chen and Miller-Hooks (2012) [42] provide an indicator for resilience that quantifies the ability of an intermodal freight network with consideration to negative consequences of disruptions resulting from topological and operational attributes. Variables used in the indicator consist of number of shipments transported and set of candidate recovery activities. Resilience is also closely tied to reduced failure probabilities, reduced consequences from failures and reduced time to recovery [43]. Vadali et al. (2015) [44] note that network disruptions used for truck routes can be approximated by several performance metrics such as travel time measures, percent of population receiving essential services and/or economic costs. And resilience has been described as the ability of the network to internalize minor perturbations. Goods and freight movement is primarily controlled by the private sector market while infrastructure facilities and maintenance is mainly the prerogative of the public agencies. Disruptions to critical networks and nodes can have potential impacts to overall freight movement and have repercussions on the commerce and the economy. Thus, the indicator of resilience should be comprehensive and be able to capture all of four components that underline resilience – robustness (ability to absorb shocks and keep operating), redundancy (back-up resources to sustain operations), resourcefulness (able to manage disruption as it unfolds), and rapidity (quickly get back to normal operations) [45].

Methodology

This research evaluates mobility and resilience of multimodal freight operations integrated with the concepts from CVT. The methodology has been spread across four broad components (called Research Emphasis) of multimodal freight operations to accomplish the following three goals:

1. Understanding constituents/factors for mobility and resilience of multimodal freight operations
2. Determining efficient routes for mobility and resilience with connected vehicles' network reliability, and
3. Estimating economic costs for CVT-induced route guidance for mobility and resilience

And the four research emphasis areas are:

RESEARCH EMPHASIS 1: Developing mobility and resilience indicators of links and nodes in a multimodal freight network, and further extending the indicators to generate path mobility and resilience.

RESEARCH EMPHASIS 2: Developing connected vehicles' network reliability model for route guidance and further insights into multimodal freight operations, and

RESEARCH EMPHASIS 3: Developing route mobility attributes connecting multimodal freight entities

RESEARCH EMPHASIS 4: Estimating economic costs for CVT-induced route guidance for mobility and resilience.

RESEARCH EMPHASIS 1: Mobility and Resilience Indicators

The information compiled in Table 2 provides the background necessary for developing mobility and resilience indicators. With the information supplied, mobility and resilience indicators are developed.

Formulation Set-up

Consider the continuous freight movement along the route segment A-B shown in Fig. 1, with exits (or route options for freight vehicle, rail etc.) as marked along the segment. One or more of

links contribute to the continuity of this freight movement. In the sketch of Fig. 1, *n* number of individual links and *n* number of nodes at each exit point diverging away from the freight movement make up the length A-B of the segment. Every link has a beginning and an ending node. The ending node of one link serves as the beginning node of its immediate following link along the traffic direction as shown using arrows in the sketch.

Table 2: Factors for mobility and resilience indicators for links and nodes of multimodal freight network

	Commercial Trucks	**Freight Rail**	**Seaports**	**Airport**
Network infrastructure element	Link	Link	Node	Node
Mobility factors	Connectivity and accessibility to seaport, airport and rail line; link speed; link truck tonnage	Connectivity and accessibility to truck routes, airport and seaport; speed of the rail; volume of rail freight tonnage on the link	Connectivity and accessibility to truck routes, airport and rail line; speed of ship travel; volume of empty/full containers handled at the port	Connectivity and accessibility to truck routes, seaports and rail line; speed of travel; air cargo volume handled at the airport
Resilience factors	Number of lanes; shoulder lane widths for emergency parking; duration of congestion; crash frequency; age of infrastructure, number of bridges; presence of railroad crossings and traffic signals; neighboring links and nodes exhibiting similar infrastructure features; crash frequency; proximity to traffic management services; proximity to parking spaces for trucks; accessibility to ramp exits/entrances; earmarked evacuation routes; presence of frontage/access/service roads; actuated traffic signals; ramp metering for freeways etc.	Length of parallel tracks with interchanges; crash data at railroad crossings; age of rail tracks and bridges; intermodal stations; presence of rail crossings and bridges; presence of staging yards; signal types on lines; number of intermodal terminals; yard capacity; distance between freight stations; parking facility for rail; accessibility to yards; freight stations; presence of dual or parallel tracks etc. [46]	Channel depth; waterfront; presence of sufficient number of on-dock rail and near dock rail; land-side connections to seaports; efficient intermodal connectors; proximity neighboring ports; number of shipping terminals; extent of waterfront; multiple on-dock rail; near dock rail; maritime area etc. [47]	Space for cargo facilities at airport; number of gate available; number of nearby airports handling air cargo; and other factors.

Mobility Indicator Formulation

In this research, mobility of a link/node is assumed to be dependent on two factors – (i) tonnage carried via the link/node due to the freight movement, and (ii) the travel time of the freight vehicle on the link to reach its ending node. Each link *i* on the roadway facilitates movement of freight tonnage value, denoted by $x_{i,k}$, for freight type *k* and the travel time incurred in the movement at time *t* being denoted by $\tau_{i,t,k}$.

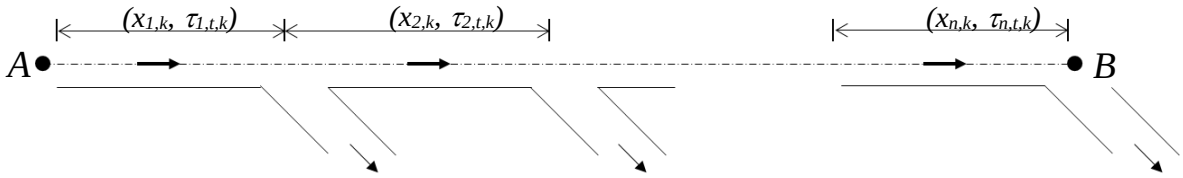

Figure 1: Sketch of roadway segment with ramp exits.

Thus, the link's mobility, $l_{i,k}(t)$, for freight type *k* (whether highway, rail line etc.) and under 'observed' traffic conditions (could be free-flow, congested, transitional etc.), is defined as follows:

$$l_{i,k}(t) = \frac{x_{i,k}}{\left(\tau_{i,t,k}\right)^{\beta}} \qquad (1)$$

where,

$x_{i,k}$ = tonnage on link *i*, for freight type *k*

$\tau_{i,t,k}$ = the travel time on the link at time *t*, for freight type *k*

β is the decay parameter (needs to be calibrated for the link or the segment)

Under 'ideal' conditions of free-flow traffic movement, the link's mobility, $L_{i,k}(t)$, carrying similar tonnage value is defined as follows:

$$L_{i,k}(t) = \frac{x_{i,k}}{\left(\Gamma_{i,t,k}\right)^{\beta}} \tag{2}$$

where, $\Gamma_{i,t,k}$ is the free flow travel time along the link at time *t*, and other parameters are as defined under 'observed' traffic conditions.

Therefore, the mobility indicator for the link, $\mu_{i,t,k}$, can be expressed as the ratio of the mobility under 'observed' traffic conditions over the mobility under 'ideal' traffic conditions:

$$\mu_{i,t,k} = \frac{l_{i,k}(t)}{L_{i,k}(t)} = \frac{\frac{x_{i,k}}{\left(\tau_{i,t,k}\right)^{\beta}}}{\frac{x_{i,k}}{\left(\Gamma_{i,t,k}\right)^{\beta}}} \tag{3}$$

A node is considered to be the end point and thus, part of the link. Therefore, the mobility of a node is same as that of its link of which it is considered to be the end node. This makes the mobility indicator of the node to have the same formula as shown in Eqn. (3).

It is often useful to derive mobility of a cluster of links or the entire path such as the segment A-B, especially applicable for long haul freight movements that involve encountering numerous links and nodes. Thus, the mobility of the roadway A-B at time *t*, $m_{n,k}(t)$, under 'observed' traffic situation, can be expressed as

$$m_{n,k}(t) = \sum_{i=1}^{n} \frac{x_{i,k}}{\left(\tau_{i,t,k}\right)^{\beta}} \tag{4}$$

where, *n* = number of links on the path from link *i* = 1 to link *i* = *n* and other factors as defined in link/node mobility equations earlier. Similarly, for the 'ideal' (or free-flow) traffic situations, the mobility of the link for freight movements at time *t*, $M_{i,k}(t)$, can be expressed as,

$$M_{i,k}(t) = \sum_{i=1}^{n} \frac{x_{i,k}}{\left(\Gamma_{i,t,k}\right)^{\beta}} \tag{5}$$

where, $\Gamma_{i,t,k}$ being the free flow travel time along the link at time *t*. Therefore, the mobility indicator for the segment from A to B, as shown in Fig. 1 at time *t*, $\Theta_{n,k}$, can be expressed as the ratio of the path's mobility under 'observed' traffic conditions over 'ideal' traffic conditions of the segment and can be written as:

$$\Theta_{n,k,t} = \frac{m_{n,k}(t)}{M_{n,k}(t)} = \frac{\sum_{i=1}^{n} \frac{x_i}{\left(\tau_{i,t,k}\right)^{\beta}}}{\sum_{i=1}^{n} \frac{x_i}{\left(\Gamma_{i,t,k}\right)^{\beta}}} \qquad (6)$$

where, the parameters in Eqn. (6) are as defined in earlier formulations.

Resilience Indicator Formulation

The formulation of resilience indicator for link/node is derived by assuming that node B in sketch of Fig. 1 is a congested point or a crash location. The aim of the freight vehicle is then to use one of the exit locations and avoid node B considering it to be the point where all vehicles are stagnant with no movement due to the jam. While a mobility indicator developed earlier reflects the level of congestion on the link/node, a resilience indicator will signify ability of the link/node to absorb shocks or disruptions and continue to assist in multimodal freight operations. The four components of resilience - robustness (ability to absorb shocks and keep operating), redundancy (back-up resources to sustain operations), resourcefulness (able to manage disruption as it unfolds), and rapidity – are inherent in the ability of freight vehicle to be able to escape or avoid locations on its route segment that are congested or could potentially cause delay or further disruption in the movement. Thus, it is vital that exit points (as exit ramps in case of freeways) en-route to destination are available at strategic locations along the freight movement path. Further, resilience of the freight movement is ensured by the time consumed in trying to circumvent the congested location on its pre-selected path that is supposedly going to be abandoned or revised. Therefore, the resilience of a node/link should depend on the travel time incurred in reaching out to the nearest exit on the segment A-B in Fig. 1. This should be coupled with the choice of the exit chosen. With this understanding, the resilience of the link, $r_{i,k}(t)$, under 'observed' traffic conditions can be expressed as:

$$r_{i,k}(t) = \frac{1}{\left(\tau_{i,t,k}\right)^{\beta}} \times \left(\frac{\exp\left(-\alpha \tau_{i,t,k}\right)}{\sum_{i=1}^{n} \exp\left(-\alpha \tau_{i,t,k}\right)} \right) \quad (7)$$

where,

α is the parameter controlling dispersion in choice of the exit, and $\tau_{i,t,k}$ = the travel time on the link at time *t*, for freight type *k.*

The term $\left(\frac{\exp\left(-\alpha \tau_{i,t,k}\right)}{\sum_{i=1}^{n} \exp\left(-\alpha \tau_{i,t,k}\right)} \right)$ in Eq. (7) represents the probability of choice of the link with an exit that has the travel time $\tau_{i,t,k}$. The higher the travel time on a link, the lesser the probability of it being selected for travel, implying a low resilience.

The exit nodes on the segment can also be used for accessing traffic management services, ramp exit/entrance points, parking space locations etc.

The equation for resilience of link, $R_{i,k}(t)$, for 'ideal' traffic situation can be written as:

$$R_{i,k}(t) = \frac{1}{\left(\Gamma_{i,t,k}\right)^{\beta}} \times \left(\frac{\exp\left(-\alpha \Gamma_{i,t,k}\right)}{\sum_{i=1}^{n} \exp\left(-\alpha \Gamma_{i,t,k}\right)} \right) \quad (8)$$

where, $\Gamma_{i,t,k}$ is the free flow travel time along the link at time *t*. The resilience indicator for the link, $\psi_{i,k,t}$, is the ratio of the link resilience for 'observed' traffic condition over 'ideal' traffic condition and is expressed as:

$$\psi_{i,k,t} = \frac{r_{i,k}(t)}{R_{i,k}(t)} = \frac{\dfrac{1}{\left(\tau_{i,t,k}\right)^{\beta}} \times \left(\dfrac{\exp\left(-\alpha \tau_{i,t,k}\right)}{\sum_{i=1}^{n} \exp\left(-\alpha \tau_{i,t,k}\right)} \right)}{\dfrac{1}{\left(\Gamma_{i,t,k}\right)^{\beta}} \times \left(\dfrac{\exp\left(-\alpha \Gamma_{i,t,k}\right)}{\sum_{i=1}^{n} \exp\left(-\alpha \Gamma_{i,t,k}\right)} \right)} \tag{9}$$

The resilience, $\delta_{i,t,k}$, of the entire segment from A to B consisting of *n* links, shown in Fig. 1 for the 'observed' traffic conditions, is a cumulative expression and is given by

$$\delta_{i,t,k} = \sum_{i=1}^{n} \frac{1}{\left(\tau_{i,t,k}\right)^{\beta}} \times \left(\frac{\exp\left(-\alpha \tau_{i,t,k}\right)}{\sum_{i=1}^{n} \exp\left(-\alpha \tau_{i,t,k}\right)} \right) \tag{10}$$

Similarly, the resilience of the segment from A to B under 'ideal' traffic conditions is:

$$\Delta_{i,t,k} = \sum_{i=1}^{n} \frac{1}{\left(\Gamma_{i,t,k}\right)^{\beta}} \times \left(\frac{\exp\left(-\alpha \Gamma_{i,t,k}\right)}{\sum_{i=1}^{n} \exp\left(-\alpha \Gamma_{i,t,k}\right)} \right) \tag{11}$$

where, $\Gamma_{i,t,k}$ is the free flow travel time along the link at time *t*. The resilience indicator, $\psi_{i,k,t}$, for the segment A-B, therefore, is the ratio of $\delta_{i,t,k}$ over $\Delta_{i,t,k}$ and is given by,

$$\psi_{i,k,t} = \frac{\delta_{i,t,k}}{\Delta_{i,t,k}} = \frac{\sum_{i=1}^{n} \dfrac{1}{\left(\tau_{i,t,k}\right)^{\beta}} \times \left(\dfrac{\exp\left(-\alpha \tau_{i,t,k}\right)}{\sum_{i=1}^{n} \exp\left(-\alpha \tau_{i,t,k}\right)} \right)}{\sum_{i=1}^{n} \dfrac{1}{\left(\Gamma_{i,t,k}\right)^{\beta}} \times \left(\dfrac{\exp\left(-\alpha \Gamma_{i,t,k}\right)}{\sum_{i=1}^{n} \exp\left(-\alpha \Gamma_{i,t,k}\right)} \right)} \tag{12}$$

Optimizing Mobility and Resilience for General Routes

The mobility of a link/node is assumed to be dependent on two factors – (i) tonnage carried via the link/node due to the freight movement, and (ii) the travel time of the freight vehicle on the link to reach its ending node. Resilience is dependent on the ramp choice aimed to avoid disruptions. The sketch in Fig. 2 illustrates the location of *n* ramps on a simplified freeway segment when trucks travel from A to B. The purpose of the sketch is to derive an optimal number of ramps, *n*, that could potentially maximize mobility of the trucks. The area around the freeway is called as freight service zones in this analysis. Thus, the service area is divided into *n* service zones each with width *W* and a constant spacing of *d* between two ramps. The freeway has a length of *L* and the theoretically simplified set-up is shown in the sketch of Fig. 2.

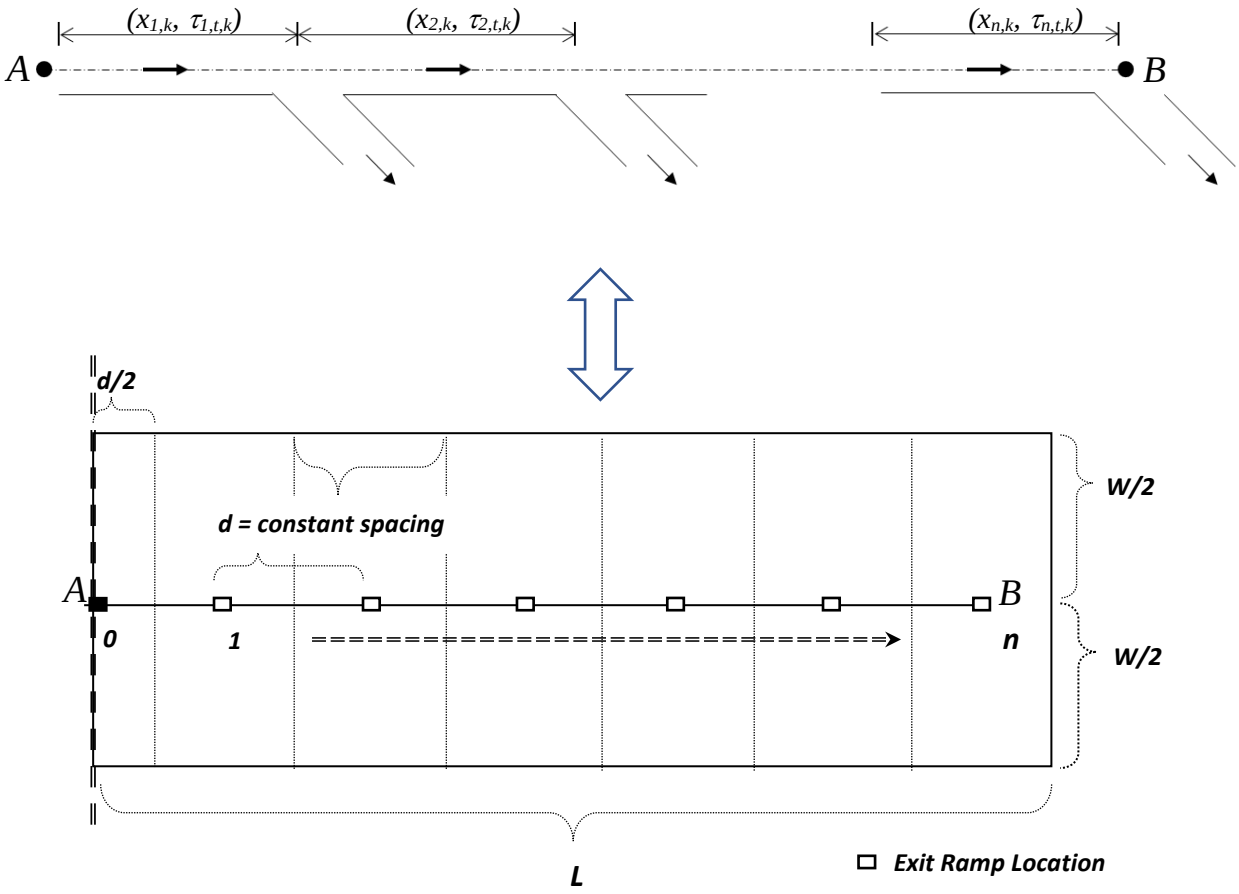

Figure 2: Freeway segment with ramp locations

Both the mobility and resilience for a route are optimized for the given set-up as shown in Fig. 2. The optimization is carried out with respect to number of ramps in the area. These are derived in detail in Appendix for different range of impedance decay factor (β) values. Table 3 summarizes these analytical findings and the corresponding mobility with various number of exit ramps (n).

Table 3: Mobility and optimal n (i.e. n^*) estimation with decay factor (β).

Impedance Decay Factor (β)	***Route Mobility***	***n****
$0 \leq \beta < 1$	$\dfrac{\rho_1 W d}{\left\{\left(\dfrac{nd}{2V}\right)+\left(\dfrac{W+d}{4v}\right)\right\}^{\beta} \Big/ (n-1)}$	*NA*
$\beta = 1$	$\dfrac{\rho_1 W d}{\left\{\left(\dfrac{nd}{2V}\right)+\left(\dfrac{W+d}{4v}\right)\right\} \Big/ (n-1)}$	Infinite
$\beta > 1$	$\dfrac{\rho_1 W d}{\left\{\left(\dfrac{n^* d}{2V}\right)+\left(\dfrac{W+d}{4v}\right)\right\}^{\beta} \Big/ (n^*-1)}$ **(Maximized)**	$\dfrac{\beta + 2\left(\dfrac{W+d}{4d}\right) \Big/ \left(\dfrac{v}{V}\right)}{(\beta-1)}$

NA= Not Applicable

Table 4: Resilience and optimal n (i.e. n^*) estimation with decay factor (β).

Impedance Decay Factor (β)	***Route Resilience***	***n****
For any β	$\dfrac{1}{\left\{\left(\dfrac{nd}{2V}\right)+\left(\dfrac{W+d}{4v}\right)\right\}^{\beta}}$	*Any $n>0$*

Optimizing Mobility and Resilience for CVT-induced Routes

With an example of freight routes, it is expected that a truck would avoid a congested point on a route by utilizing CVT-based information. Thus, the volume on the given link of congestion should decrease minimizing that link's travel time based on the standard Bureau of Public Roads (BPR)-type function [48]:

$$t_a = t_a^0\left[1+0.15\left(Q/y\right)^4\right] \tag{13}$$

where, t_a denotes the average travel time of the study road segment a, t_a^0 denotes the free-flow travel time, and Q, y are the aggregated traffic flow and road capacity in passenger car units. Thus, with decrease in Q or the freight truck flow, there will be observed increase in route mobility and resilience due to lowering in travel times.

Summary of Findings and Implications

Route Context: The theoretical indicators developed and presented above in Eq. (6) and (12) are time-sensitive and vary between 0 and 1. This assists in easy interpretation in the multimodal context. Thus, an indicator value of 0 denotes poor or low mobility/resilience and a value of 1 denotes high mobility/resilience of a route/path being examined. Alternatively, a mobility indicator value of 0 would signify a highly congested route and a value of 1 would indicate free-flow conditions prevailing along the route for a given time of the day.

Link/Node Context: A resilience indicator value of 0 would mean an extremely vulnerable link/node and a resilience value of 1 would indicate a highly resilient link/node of the multimodal freight network. Due to indicators being time-sensitive, both the mobility and the resilience indicators would vary temporally during the day.

For simplicity, in this report, the formulations are developed to cause the indicators to vary between 0 and 1, and hence, a factor of 100 can be multiplied to all the equations of mobility and resilience indicators between 0 and 100.

The decay parameter, β, and the parameter, α, controlling dispersion in choice of the exit are estimate based on the travel time data collected for approximately 11 to 15-mile continuous stretch of various interstates in the Southern California Region. These interstates are I-405, 10, I-710 and I-10 (see map in Fig. 3).

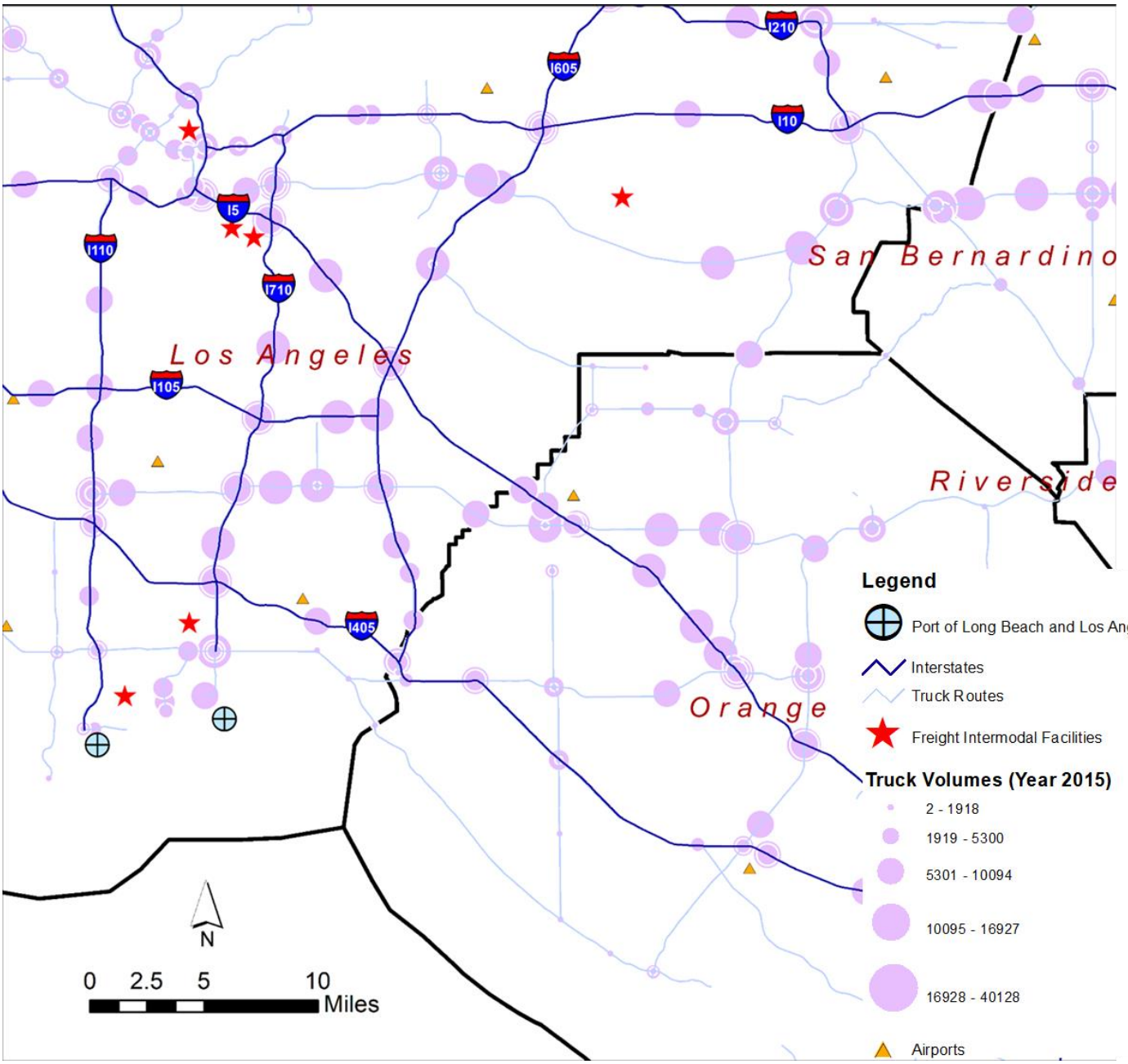

Figure 3: Multimodal infrastructure used for the application of mobility and resilience indicators.

The tonnage values for each of the links constituting the 11 to 15-mile length are obtained from the year 2012 Freight Analysis Framework (FAF) data [49].

The travel time data along with tonnage information for the links are used for estimating the value of parameter β. The travel time information is obtained from 2015 travel demand model data provided by the Southern California Association of Governments (SCAG) and corroborated with data from the Google Maps. For simplicity, the data are documented for the time period between 6:00 am to 6:00 pm- which includes the peak period of traffic for trucks. These are provided in detail under Appendix.

Based on the calibration using these data, preliminary results for parameter values are being shown in Table 5.

Table 5: Estimates for parameter (β)

Interstate	**β-value**
I-405	5.896
I-5	11.11
I-10	7.5
I-710	12

Irrespective of the highway analyzed, the value of parameter α can be assumed to be 1. A more accurate value of α, however, can only be obtained using data on route detours and deviations using a simulation model, which will be part of future work.

The mobility and the resilience indicators will differ for the 'with CVT' and 'without CVT' case only due to changes in volume. It is expected that vehicles 'with CVT' will reschedule or reroute their paths to avoid congested points of a highway, thus reducing volumes on perpetually congested links. Reduction in volumes for these links would also lead to reduction in each link's travel time, as evident from the BRP function of Eq. (13).

Thus, the mobility and the resilience indicators shown in Table 6, systematically improve for the 'with CVT' case when compared with the 'without CVT' case for percentage reductions in volumes experienced at individual links of the routes on I-405, I-5, I-10 and I-710. The truck volume data are obtained for the year 2015 from Caltrans GIS Data Library [50]. The value of α is assumed to be equal to 1.

However, for dense traffic conditions these indicators actually do not change much with the influence of CVT. This could be due to limited route options for trucks to deviate during situations when the traffic is dense.

Table 6a: Compilation of CVT-induced routes on some popular freeways in Southern California Region

Freeway	**Mobility Indicators (in**				**Resilience Indicators**			
	Without CVT	**With CVT (Trucks sharing lane with general traffic)**			**Without CVT**	**With CVT (Trucks sharing lane with general traffic)**		
		% Volume Reduction w.r.t. Without CVT				*%* Volume Reduction w.r.t. Without CVT		
		10	*20*	*30*		*10*	*20*	*30*
I-405	0.031	0.033	0.040	0.049	0.0040	0.0042	0.0052	0.006
I-5	0.002	0.003	0.0041	0.0047	0.0002	0.0003	0.00039	0.00047
I-10	0.001	0.0016	0.0022	0.003	0.0947	0.097	0.102	0.2
I-710	0.041	0.052	0.065	0.071	0.0162	0.023	0.036	0.042

Table 6b: Percentage change in the mobility and resilience indicators

Mobility Indicator Changes (%) ('with CVT' - 'without CVT')*100/ 'without CVT'				Resilience Indicator Changes (%) ('with CVT' - 'without CVT')*100/ 'without CVT'			
I-405	6	29	58	**I-405**	5	30	50
I-5	50	105	135	**I-5**	50	95	135
I-10	60	120	200	**I-10**	2	8	111
I-710	27	59	73	**I-710**	42	122	159

Based on the information compiled in Table 6a, it is noted that the indicator values do not change much for the change in percentage volume of traffic (comprising both passenger and freight truck) and also do not capture any peak or non-peak hours of travel on the routes selected for analysis. However, slight increase in the mobility and resilience indicators are noted for drop in volume of traffic which helps freight trucks navigate on the respective routes.

It is also noted that for the length of the segments selected for the routes, I-10 appears to be worst in terms of the mobility indicator, while ranks better than all the routes in terms of the resilience indicator. I-710 appears to be having much better mobility as compared to rest of the

routes. This could be due to high truck volumes experience on the interstate resulting in large total tonnage value. Note that all these interstates connect one or more intermodal terminals and ports in the Southern California Region. However, in general, most of the interstates appear to be having overall low values of mobility and resilience as reflected in low values of the indicators in Table 6a. However, Table 6b shows that I-10 is expected to experience the largest percentage increase in mobility and I-710 would have the largest percentage increase in resilience with the implementation of CVT.

These values of mobility and indicator obtained here can be used in future as elements to design Connected Vehicle Technology or Intelligent Transportation System where rerouting of vehicles will be necessary to produce an efficient freight network.

RESEARCH EMPHASIS 2: Reliability Modeling

The network reliability model and analysis is based on concepts borrowed from percolation theory. Percolation is the polymerization process of molecules that lead to large network formations through chemically connected bonds [51]. In literature, the classical percolation theory is related to bond percolation and site percolation problem ([52], [53]). The bond percolation problem consists of bonds being occupied with certain probability which would ultimately provide connectivity across a given media. A connection is established between two sites if a bond exists between them and the site is said to be an occupied bond. However, if a bond is occupied, it is quite likely that the adjacent bonds which are immediate neighbors have an increased chance of being occupied as well. When several such connections are established collectively among a group of bonds surrounded by empty or unoccupied bonds, it is called a 'cluster'. A cluster formation is completely random. The image in Fig. 3 shows the bond cluster formation in a 25×25 square lattice during a 2D percolation process. The bonds are occupied with probability p= 0.335 in Fig. 4(a) and p = 0.525 in Fig. 4(b) (Source: Albert and Barabási, [54]). Thus, a bond describes the connectivity between sites and the bond percolation, therefore, can be considered as the reliability of the connectivity among sites.

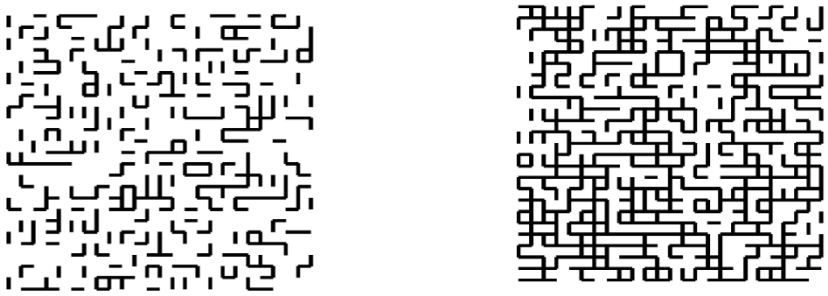

(a) (b)

Figure 4: Bond cluster formation in 2D. Nodes places in a 25×25 square lattice and two nodes connected by a bond with probability p, (a) $p = 0.335$ (b) $p = 0.525$.

In literature, the study of percolation is generally subdivided into discrete and continuum models. The discrete percolation model investigates any cluster of infinite size with probability 1 if $p>\sigma_c$ (for σ_c being the critical density) and for $p<\sigma_c$, this probability is zero [55]. For a multimodal transportation, the network reliability resulting from percolation is analogous to probability of communication between individual freight vehicles interacting with other freight vehicles, ports, railroad infrastructure and the intermodal stations. In this research, we use the concept of continuum model (as an extension of discrete percolation model) to construct connectivity among series of freight trucks, rail, ship, air cargo, ports and intermodal facilities through wireless sensor networks in a two-dimensional percolation problem.

The model presented by Talebpour et al. (2017) [56] on correlation between communication range and connected vehicles density (shown in Fig. 5) is extended to develop connected component along a highway segment of length, L, for freight trucks, instead of cars. A theoretical framework is first established for the continuum percolation model. The reason for adopting a continuum model is that individual communicating trucks are connected through a series of circular overlapping sensor transmission range of radius, R, for each freight vehicle in a multimodal transportation operation. For the purpose of simplicity, each vehicle, having a sensor, is assumed to have a disk-shaped transmission range surrounding its location at a given time, t. In general, as the transmission range from one vehicle overlaps with the transmission range of another vehicle, continuity of communication occurs.

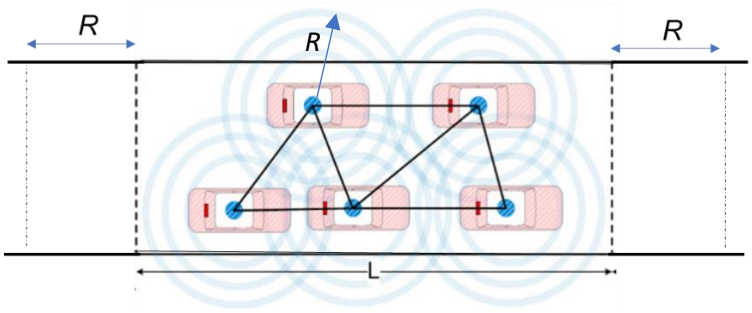

Figure 5: Connected component along a highway segment (Source: Talebpour et. al (2017) [56])

The analysis is carried out for CVT evaluation among multimodal freight vehicles which are neighbors in the area and the exchange of information is said to occur at the 'micro-level'. Two freight vehicles are considered 'neighbors' if they belong to the same cluster as determined for analysis, and are interacting with each other by intersecting circular discs of radii equal to the sensor transmission range of each vehicle. Thus, only a limited number of vehicles which are neighbors are of focus at the micro-level analysis.

When the analysis is carried out for CVT evaluation among non-neighboring multimodal freight vehicles, this is conceptualized as information exchange occurring at a 'macro-level'. Thus, at a macro-level, the CVT-based information exchange can span interactions among multimodal freight entities across the entire stretch of a given freeway or among vehicles belonging to different clusters. Macro-level analysis involves focusing on interactions among much larger number of vehicles than at the micro-level.

At critical density, σ_c, an unbroken chain of information exchange occurs among vehicles for the first time in the network having *N* vehicles. The information exchange could be on mobility and resilience of transportation network's links (and nodes) through sensor transmissions. Interpreted in mathematical terms, connectivity of information in the network is non-existence for number of vehicles (having no sensor transmissions) equal to $\left(N - N\sigma_c\right)$. With $\left(N\sigma_c + 1\right)$ minimum number of vehicles connected through communication of sensor transmissions in the cluster and subsequently, the network reliability at macro-level $R_M\left(t\right)$ at time *t*, based on critical percolation is given by:

$$R_M(t) = \sum_{i=(N\sigma_c+1)}^{N} \binom{N}{i} r_m(t)^i \left(1 - r_m(t)\right)^{N-i} \tag{14}$$

where, $r_m(t)$ is the network reliability within a given cluster from at the micro-level at time *t*. Physically, this is illustrated using cluster interactions at micro and macro-level of Fig. 6. The formula for the macro-level reliability expressed in Eq. (14) is based on the model of voting system [57].

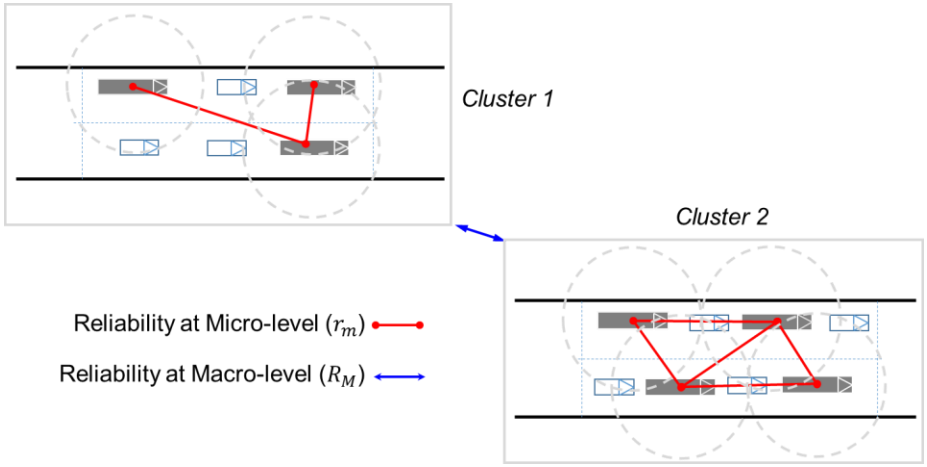

Figure 6: Illustration of reliability at the micro and macro level.

The reliability, $r_m(t)$, of communication at micro-level within a cluster of freight trucks communicating with each other can be considered to have varying sensor transmission probability distributions, known as lifetime distributions. Li et al. [57] used three different lifetime distributions for micro-level, reliability as shown below:

1. *Exponential distribution*: $r_m(t) = \exp(-\lambda t)$, where λ is the scale parameter.
2. *Uniform distribution*: $r_m(t) = \dfrac{(b-t)}{(b-a)}$, where *a*, *b* are the lower and upper limits of the interval, respectively.

3. *Weibull distributions*: $r_m(t) = \exp\left(-\left(\frac{t}{\lambda}\right)^k\right)$, where λ, k are the scale parameter and shape parameter, respectively.

Summary of Findings and Implications

Although the findings can be explained only at a theoretical level at this point, the idea is simple - as the reliability at the micro-level among a cluster of vehicle increases so does the overall reliability of communication among several 'mini' clusters.

For example, consider the micro-level reliability, $r_m(t)$, of communication within a cluster will be a probability varying between 0 and 1. Thus, the reliability, $R_M(t)$, at the macro-level using the reliability, $r_m(t)$, of communication at the micro-level for any of the three lifetime distributions mentioned above will vary as shown in the charts of Fig. 7.

The graphs in Fig. 7 have been developed for the exponential distribution of $r_m(t)$ with values of $r_m(t)$ = 0.90, 0.87, 0.85, 0.83 and 0.81, in the decreasing order as marked in Fig. 7. Thus, for decreasing values of micro-level reliability ($r_m(t)$) the macro-level reliability ($R_M(t)$) will tend to decrease as well. This can be further corroborated with the fact that a low micro-level reliability among individual vehicles of a cluster on an average will lead to low macro-level reliability of the group of clusters. Alternatively, as also evident in Fig. 5, low values of $(N\sigma_c + 1)$ and fixed *N* (total number of vehicles in the group of clusters) make the macro-level reliability vary diminish with decrease in critical density, σ_c. Lower the critical density, σ_c, higher the reliability, $R_M(t)$. This indicates that higher macro-level reliability, $R_M(t)$, occurs at a bigger size cluster of communicating vehicles due to low critical density, σ_c.

In relation to multimodal freight, a higher value of macro-level communication network reliability will be ensured if vehicle-to-vehicle communication at the micro-level is strong and with low value of critical density.

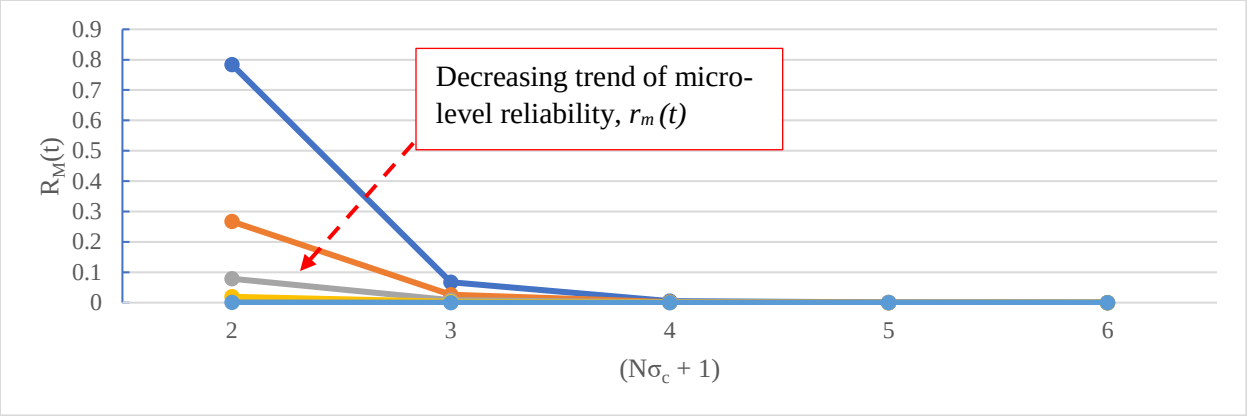

Figure 7. Macro-level reliability variation with minimum number of vehicles connected in a cluster

RESEARCH EMPHASIS 3: Multimodal Route Attributes for Connectivity

As a first step in this research emphasis, a simplified model is developed with a group of freight trucks interacting/communication through sensor transmissions with a range of influence, denoted by a disc of radius, *R*, for each freight truck. Similar, communications can be established among intermodal terminals, ports and/or airports in a multimodal freight operation, assuming that each individual entity in a multimodal system is equipped with a sensor device as expected in a CVT-setting.

In probability theory, for random uniform distribution, the instantaneous gap, δ, between any two vehicles for sparse traffic conditions (*uncongested*) is assumed to follow a Poisson distribution [58] while under dense traffic conditions (*congested*) the gap between successive vehicles is assumed to follow Gaussian Unitary Ensemble (GUE) distribution [59]. These two distributions are used to derive the expected closest between two freight vehicles on a highway segment with the set-up shown in Fig. 8.

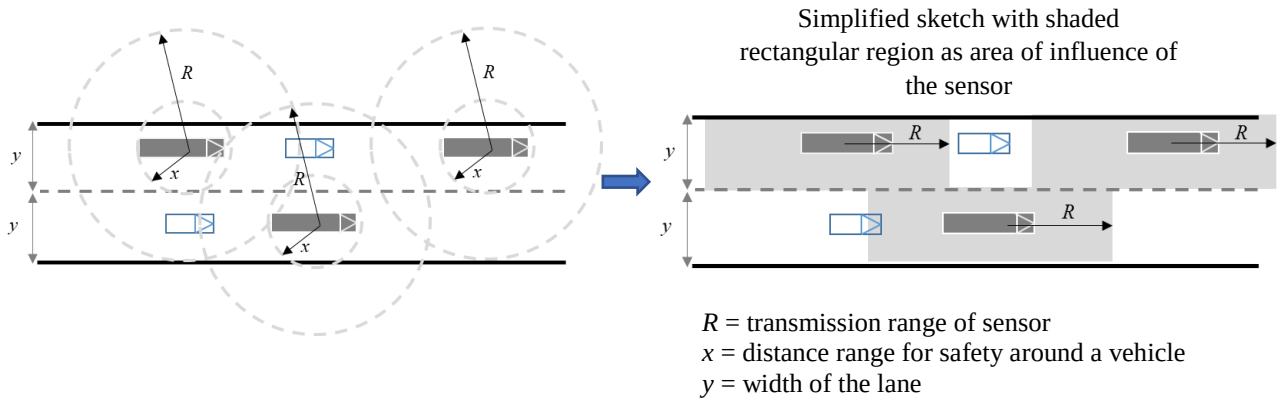

Figure 8: Set-up for expected closest distance between two freight vehicles for establishing connectivity in communication with safety against collision

The connectivity of communication between two vehicles is established if the transmission range (denote by *R*) of the censors of the two vehicles overlap (or at least touch tangentially). An assumed distance of x ($\leq R$) units ensures the closest a truck can be to another truck for safety against collision. The sketch in Fig. 6 shows the simplified version of sensor to sensor interaction for information exchange with just two lanes of the freeway. This is a valid assumption because

as observed certain states such like in California and Texas, most of the freight truck routes are required by law to use only the two-rightmost lanes of a freeway [60].

Expected Distance between Vehicles under Uncongested Conditions

As mentioned earlier with reference to Fig. 8, the spatially random uniform distribution of trucks (with density σ) on a highway segment can be expressed as a Poisson process. The expression of probability defined as the number of vehicles (say, b), within the rectangular area $2\sigma y\delta$, for a random distance δ as,

$$P(\varphi = b) = \frac{(2\sigma y\delta)^b e^{-2\sigma y\delta}}{b!} \tag{15}$$

Thus, the probability that there is no sensor transmission influence within a distance range from x to R around the freight truck with any other vehicle in the same lane (as shown in Fig. 8), is given by $P(\varphi = 0) = e^{-2\sigma y\delta}$. Therefore, the expected distance ($S_{x,R}$) between two freight trucks such that the connectivity of communication is established with overlapping sensor transmission discs of radius R is given by,

$$S_{x,R} = \int_x^R P(\varphi = 0)\, d\delta = \int_x^R e^{-2\sigma y\delta} d\delta = \frac{1}{2\sigma y}\left(e^{-2\sigma yx} - e^{-2\sigma yR}\right) \tag{16}$$

Expected Distance between Vehicles under Congested Conditions

Under dense traffic situations, the Gaussian Unitary Ensemble (GUE) distribution is given by [59],

$$f(\delta) = \frac{32y^3\delta^2\sigma^3}{\pi^2} e^{-\frac{4y^3\delta^2\sigma^2}{\pi}} \tag{17}$$

Note that the GUE distribution is a continuous probability distribution and with the density of multimodal freight components being σ, the expected spatial distance ($D_{x,R}$) between the two freight trucks using GUE distribution is given by ,

$$D_{x,R} = \int_x^R \delta f(\delta) d\delta = \int_x^R \frac{32y^3\delta^3\sigma^3}{\pi^2} e^{-\frac{4y^3\delta^2\sigma^2}{\pi}} d\delta = \int_x^R c\delta^3 e^{-v\delta^2} d\delta; \qquad (18)$$

where, $c = \frac{32y^3\sigma^3}{\pi^2}$ and $v = \frac{4y^2\sigma^2}{\pi}$

Assume, $k = \delta^2 \Rightarrow dk = 2\delta d\delta$, $\Rightarrow D_{x,R} = \int_{x^2}^{R^2} \frac{cke^{-vk}}{2} dk$

Therefore,

$$D_{x,R} = \frac{c}{2}\left[e^{-vk}\left(\frac{-vk-1}{v^2}\right)\right]_{x^2}^{R^2} = \frac{c}{2}\left[e^{-vR^2}\left(\frac{-R^2v-1}{v^2}\right) - e^{-vx^2}\left(\frac{-x^2v-1}{v^2}\right)\right]$$

$$= \frac{32y^3\sigma^3}{\pi^2}\frac{1}{2}\left[e^{-\frac{4y^2\sigma^2}{\pi}R^2}\left(\frac{-\frac{4y^2R^2\sigma^2}{\pi}-1}{\left(\frac{4y^2\sigma^2}{\pi}\right)^2}\right) - e^{-\frac{4y^2\sigma^2}{\pi}x^2}\left(\frac{-\frac{4y^2x^2\sigma^2}{\pi}-1}{\left(\frac{4y^2\sigma^2}{\pi}\right)^2}\right)\right]$$

$$\Rightarrow D_{x,R} = \frac{16y^3\sigma^3}{\pi^2}\left[e^{-\frac{4\sigma^2R^2}{\pi}}\left(\frac{-\frac{4y^2\sigma^2R^2}{\pi}-1}{\left(\frac{4y^2\sigma^2}{\pi}\right)^2}\right) - e^{-\frac{4\sigma^2}{\pi}x^2}\left(\frac{-\frac{4y^2\sigma^2x^2}{\pi}-1}{\left(\frac{4y^2\sigma^2}{\pi}\right)^2}\right)\right]$$

$$D_{x,R} = \frac{1}{y\sigma}\left[\left(\frac{4y^2\sigma^2x^2}{\pi}+1\right)e^{-\frac{4y^2\sigma^2}{\pi}x^2} - \left(\frac{4y^2\sigma^2R^2}{\pi}+1\right)e^{-\frac{4y^2\sigma^2R^2}{\pi}}\right] \qquad (19)$$

Expected Distance between Intermodal Station and First Closest Freight Vehicle – Sparse Traffic Condition

An intermodal transfer station is assumed to be connected with its surrounding infrastructure and senses any freight vehicle (truck, rail, ship or air cargo) that is within a radius *H* around the terminal centroid as shown in the left-hand side image of Fig. 9. The distribution of vehicles follows a Poisson process with the expected value σA_H , where σ is the spatial density of the distribution of freight vehicles (such as trucks) and A_H is the area approximated as a rectangle surrounding the intermodal terminal. The variable *H* in the right-hand side image of Fig. 9 is the distance between the terminal and the boundary touching the area of influence of the sensor transmitted from the closest freight truck. Thus, $A_H = 2YH$.

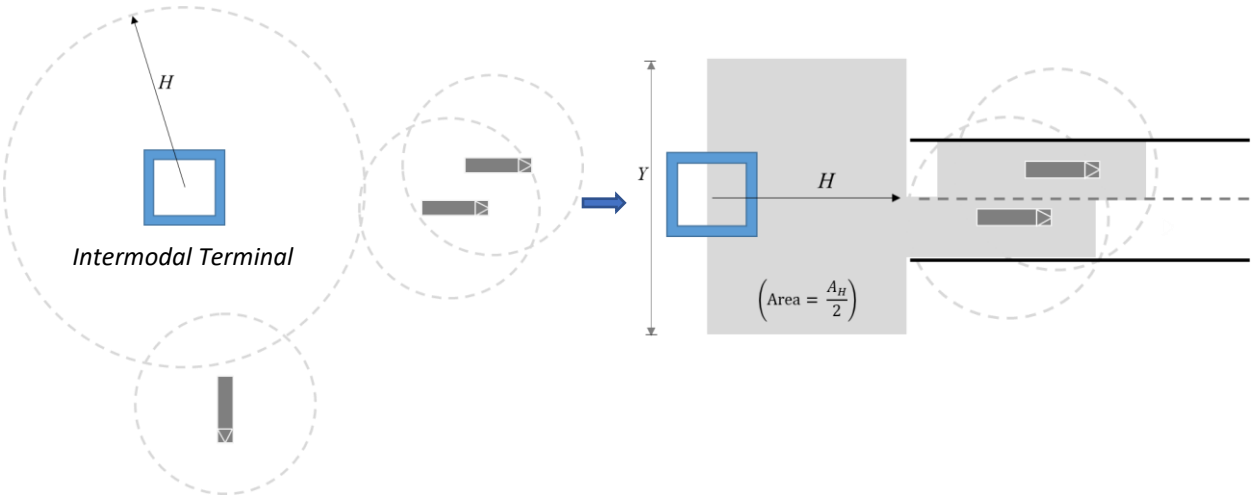

Figure 9: Set-up for derivation of expected closest between intermodal terminal to nearest vehicle

The probability of finding *c* number of freight vehicle within an area $(A_H / 2)$ towards the freeway lane to the right is,

$$P(c=b) = \frac{\left(\frac{\sigma A_H}{2}\right)^b e^{-\frac{\sigma A_H}{2}}}{b!} \qquad (20)$$

where, σ = density of freight vehicle and b = 0, 1, 2, …

The average closest distance ($E[H]$) between the terminal and a freight vehicle can be obtained for b=0, where Y is the total width of the area surrounding the terminal that is a rectangular coverage of the sensor as it advances towards the lanes to the right.

$$E[H] = \int_0^\infty e^{-\frac{\sigma A_H}{2}} \mathrm{dH} = \int_0^\infty e^{-\sigma Y H} \mathrm{dH} = \frac{1}{\sigma Y} \tag{21}$$

Expected Distance between Intermodal Station and First Freight Vehicle – Dense Traffic Condition

For the dense traffic condition, we use the Gaussian Unitary Ensemble (GUE) distribution as shown in Eq. (17). The average closest distance ($E[G]$) between the terminal and a freight vehicle can be obtained as follows:

$$E[G] = \int_0^\infty \delta f(\delta) d\delta = \int_0^\infty \frac{32Y^3\delta^3\sigma^3}{\pi^2} e^{-\frac{4Y^3\delta^2\sigma^2}{\pi}} d\delta = \int_0^\infty C\delta^3 e^{-V\delta^2} d\delta;$$

where, $C = \frac{32Y^3\sigma^3}{\pi^2}$ and $V = \frac{4Y^2\sigma^2}{\pi}$

Assume, $K = \delta^2 \Rightarrow dK = 2\delta d\delta$, $\Rightarrow E[G] = \int_0^\infty \frac{CKe^{-vK}}{2} dK$

Therefore,

$$E[K] = \frac{C}{2}\left[e^{-VK}\left(\frac{-VK-1}{V^2}\right)\right]_0^\infty = \frac{C}{2V^2} = \frac{32Y^3\sigma^3}{2\pi^2\left(\frac{4Y^2\sigma^2}{\pi}\right)^2} = \frac{1}{\sigma Y} \tag{22}$$

Average cluster size for communication connectivity

Consider cluster size of connected *k*-components (or, *k* number of freight trucks) with identical sensor transmission range of each component equal to *R*. The probability that there is exactly one connected *k*-component in the length of highway segment equal to *L* having density of vehicles with sensor transmissions equal to σ, is derived by Talebpour et al. [56] as:

$$P(N=k)=\frac{\lceil \sigma(L+2R) \rceil^{k}}{k!}e^{-\sigma L} \tag{23}$$

Extending the findings in Eq. (23), the average size (*M*) of the connected *k*-component can be obtained using the following expression,

$$E[M]=\sum_{k=0}^{N} k\frac{\lceil \sigma(L+2R) \rceil^{k}}{k!}e^{-\sigma L} \tag{24}$$

For very large *N*, almost equal to infinity, Eq. (24) can be modified as,

$$\begin{aligned}
E[M] &\approx \sum_{k=1}^{\infty}\frac{\lceil \sigma(L+2R) \rceil^{k}}{(k-1)!}e^{-\sigma L} \\
&= \sigma(L+2R)e^{-\lambda L}\sum_{k=1}^{\infty}\frac{\lceil \sigma(L+2R) \rceil^{k-1}}{(k-1)!} \\
&= \sigma(L+2R)e^{-\sigma L}\left(\frac{\lceil \sigma(L+2R) \rceil^{0}}{0!}+\frac{\lceil \sigma(L+2R) \rceil^{1}}{1!}+\ldots\right) \\
&= (L+2R)e^{-\sigma L}\sum_{k=0}^{\infty}\frac{\lceil \sigma(L+2R) \rceil^{k}}{k!} \\
&= (L+2R)e^{-\sigma L}e^{\sigma(L+2R)} \\
&= (L+2R)e^{2\sigma R}
\end{aligned} \tag{25}$$

Summary of Findings and Implications

Optimum Sensor Transmission Radius

The application of the communication connectivity is demonstrated using assumed values for density of freight vehicle on a 10-mile highway segment. In this example, density below 50 veh/mile/lane is assumed to be sparse and density above 50 veh/mile/lane is assumed to be congested traffic conditions [61].

In order to obtain optimum sensor transmission range, connectivity of transmission across all vehicles on a given highway segment should be established. Thus, the number of vehicles with sensors sharing information should be able to cover the entire segment length of the highway being studied. Based on the expected distance between two freight vehicles obtained in Eq. 16 and Eq. 19 and using range of vehicle densities assumed for the highway, optimum radii of sensor transmission range are obtained. This is illustrated using the charts of Fig. 10 and Fig. 11 for Eq. 16 and Eq. 19, respectively. The charts are constructed assuming freight vehicles use only one lane of the highway.

As noted in Fig. 10, the ratio of theoretical number of vehicles with sensors to total number of vehicles on highway is almost 1 when the optimum radius of transmission range is greater than 1500 feet for traffic densities lower than 9 veh/mile (under sparse traffic conditions). This optimum radius for transmission range is higher than 55 feet for traffic densities lower than 100 veh/mile with dense traffic conditions, as shown in Fig. 11.

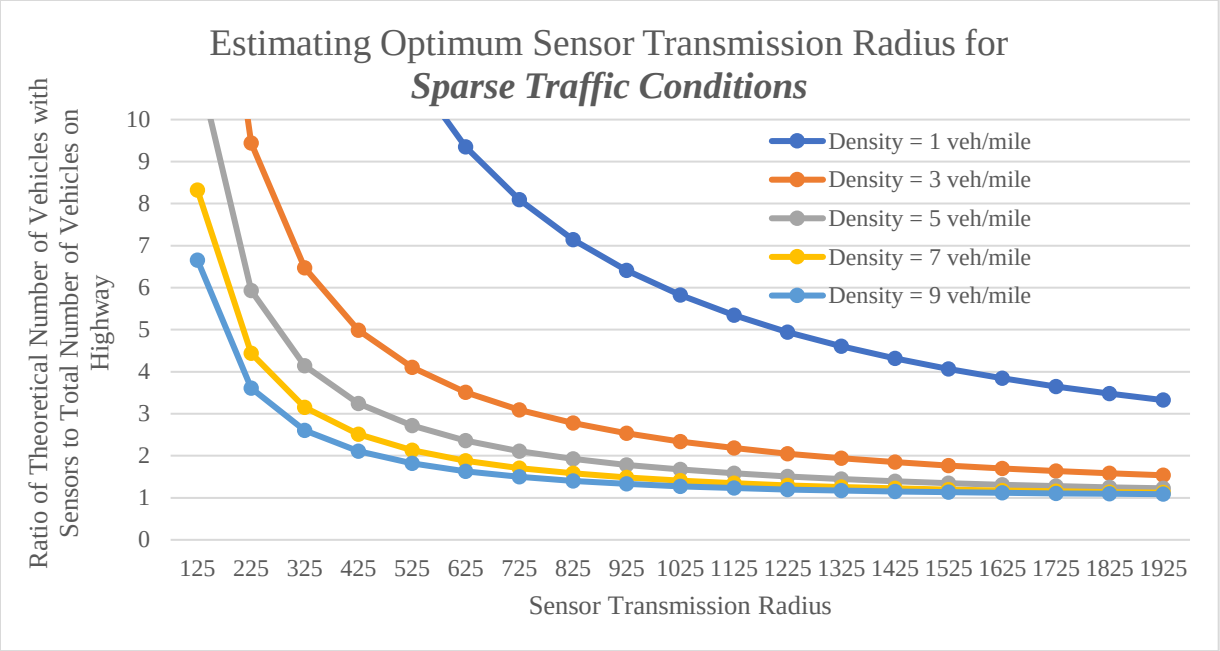

Figure 10: Estimating optimum sensor transmission radius for sparse traffic conditions

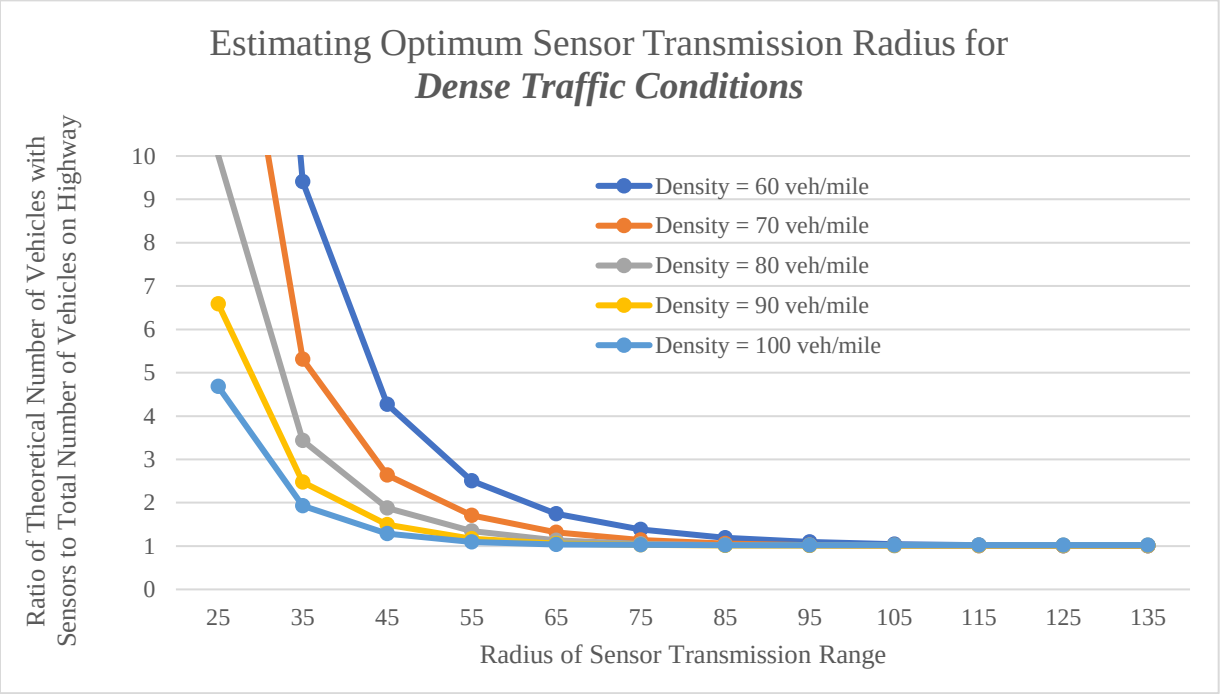

Figure 11: Estimating optimum sensor transmission radius for dense traffic conditions.

There are two other findings from this research emphasis:

1. Irrespective of the density of the freight vehicles around an intermodal terminal, port or airport (i.e. congested or uncongested highway with trucks), the expression for the average distance to the closest freight truck does not change. This is evident from the final expressions obtained in Eqs. (21) and (22).

2. Based on Eq. (23), the average or the expected size of the connected *k*-component is equal to $(L+2R)e^{2\sigma R}$ - which means that as the length of the highway segment, L, increases, there is linear increase in the average size of connected *k*-component (i.e. *k* trucks). However, there is exponential increase in the average size of the connected *k*-component (trucks) with increase in density of vehicles (σ) and/or with increase in sensor transmissions radius (R).

RESEARCH EMPHASIS 4: Costs with CVT-induced Routes

Motor carrier cost estimations were carried out for some sample routes for the 'without CVT' and the 'with CVT' case. The routes are selected such that they connect intermodal terminals to ports/airports and vice versa. These were mainly computed for the operational costs, divided into two general categories – (i) vehicle-based, and (ii) driver-based. The vehicle-based motor carried operational costs were further subdivided into fuel, truck/trailer lease or purchase payments, repair and maintenance, truck insurance premiums, permits and special licenses, and tolls. The driver-based operational costs involved wages and benefits. The data for the marginal costs were obtained for the year 2016 from the American Transportation Research Institute (ATRI) and have been compiled in Table 7 for motor carrier costs per mile and motor carrier costs per hour:

Table 7: Motor carrier costs for the year 2016 (Source: ATRI, 2017) [62]

Motor Carrier Costs	Average Marginal Costs per Mile (Year 2016)	Average Marginal Costs per Hour (Year 2016)
Vehicle-based		
Fuel Costs	$0.336	$13.45
Truck/Trailer Lease or Purchase Payments	$0.255	$10.20
Repair & Maintenance	$0.166	$6.65
Truck Insurance Premiums	$0.075	$3.00
Permits and Licenses	$0.022	$0.88
Tires	$0.035	$1.41
Tolls	$0.024	$0.97
Driver-based		
Driver Wages	$0.523	$20.91
Driver Benefits	$0.155	$6.18
TOTAL	**$1.592**	**$63.66**

The marginal costs displayed in Table 7 is based on the mean vehicle speed of 39.98 mile per hour and the average cost per mile for all sectors of motor carriers, namely - truckload (TL), less-than-truckload (LTL), and specialized fleets.

While computing the costs for routes, the operational costs per mile would not be impacted - whether for 'without CVT' or 'with CVT' case. However, savings in operational costs per hour would occur if freight trucks are moving in a platoon over a dedicated truck lane that is not impacted by interference from passenger cars.

Summary of Findings and Implications

Motor carrier costs are evaluated across the four chosen routes for analysis: I-405, I-5, I-10 and I-10. For freight trucks using these routes, shared with passenger cars, it is determined that travel times for sparse traffic without CVT and with CVT are approximately the same. Further, the data uses the difference in travel time for three categories: sparse traffic without CVT, dense traffic without CVT, and with CVT. The speed of trucks traveling during sparse traffic is nearly the free-flow speed. When using CVT, the goal is to have trucks move at this speed, whether there is sparse or dense traffic.

Tonnage is observed in relation to truck volume. By averaging the current data for tonnage and truck volume without CVT for each interstate, the ratio of kilotons per truck per year is calculated. Once the truck volume with CVT is estimated, by using the ratio from current data, the tonnage in relation to CVT is also calculated. Note that the tonnage in relation to truck volume with CVT is only an estimate to match the current ratio.

Motor Carrier Operational Costs for I-405, I-5, I-10 and I-710

Table 8 presents the data for volumes, travel distance and travel time for the individual routes that connect from one or more intermodal terminals, ports and airports. It is noticed that for the 'with CVT' case, each of the routes reach the capacity with freight truck volumes – this is deduced from the expressions for expected distance obtained from Eq. (16), Eq. (19), Eq. (21) and Eq. (22) – for sparse traffic conditions (5 veh/mile) and for congested traffic conditions (50 veh/mile). Table 8 also shows that irrespective of the traffic density, the travel time for the 'with CVT' case and 'without CVT' case is identical. This also means that freight vehicle movement is synchronized as in a platoon in dedicated lanes, without any interference from passenger vehicles on other lanes.

Table 8: Compiled freight data for routes

Freeway	Average Volume/Day/Section		Distance (miles)		Travel Time (minutes)			
	Without CVT	With CVT	Without CVT	With CVT	Without CVT		With CVT	
					Sparse Traffic	Dense Traffic	Sparse Traffic	Dense Traffic
I-405	9943	21264	30	30	33	44	33	33
I-5	8253	16104	18	18	19	30	19	19
I-10	15952	20316	28	28	30	45	30	30
I-710	16650	25164	19	19	20	25	20	20

The chart in Figs. 12 -15 shows that the average marginal cost value for the routes for the 'without CVT' case is approximately in the range of $300 to $8,000 across for the individual motor carrier cost. However, for the same costs the range is approximately between $ 400 to $11,000 for the 'with CVT' case. Thus, there is approximately a 37% increase for motor carrier operational costs for the 'with CVT' case as compared to the 'without CVT' case. The costs are computed for total truck volume for the two cases for peak hours of travel. The variation in the average marginal costs per mile for total trucks is higher for the 'with CVT' case than for the 'without CVT' case. This is because, although the travel distance on routes do not change, a higher number of freight vehicles are obtained which are near to capacity of each route for the 'with CVT' case than for the 'without CVT' case. The marginal costs are the largest for I-405 route, since the truck volumes under high freight density scenario obtained using Eq. (19) and Eq. (22) for the 'with CVT' case gives the largest number of freight vehicles.

Total motor carrier costs per hour per truck shown in Figs. 16 – 19 indicate that the values for the 'without CVT' case under sparse traffic and for the 'with CVT' case are similar. This is because the travel times incurred for the two cases are identical, as noted in Table 8. However, there is a reduction in costs for the 'with CVT' case as compared to the 'without CVT' case. This is due to an increase in travel time for the 'without CVT' case. Similar observations are made for the fuel costs per hour per truck as savings for the 'with CVT' case as compared to the 'without CVT' case evident in Figs. 20 – 23. Due to higher volumes for the 'with CVT' case, the routes experience high tonnage values with respect to the 'without CVT' case. The tonnage value is the highest for the I-405 route for the 'with CVT case', due to large number of freight trucks that can be occupy the route for the given segment lengths of the freeway used in the analysis.

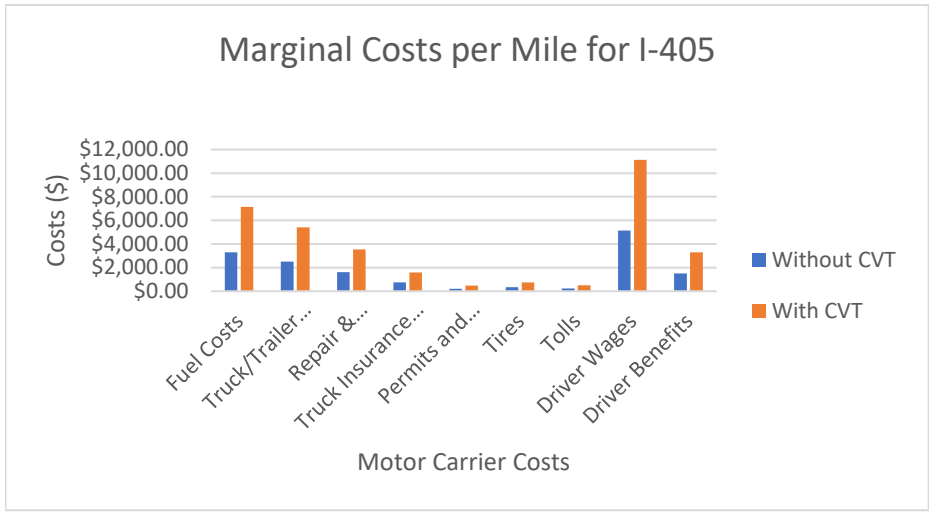

Figure 12: Comparison for marginal motor carrier operational costs for I-405 for the 'without CVT' and the 'with CVT'

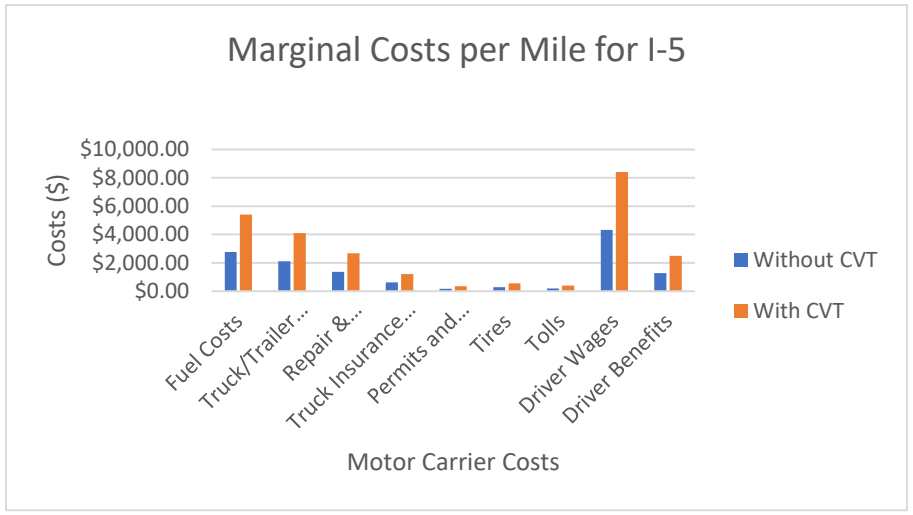

Figure 13: Comparison for marginal motor carrier operational costs for I-5 for the 'without CVT' and the 'with CVT'

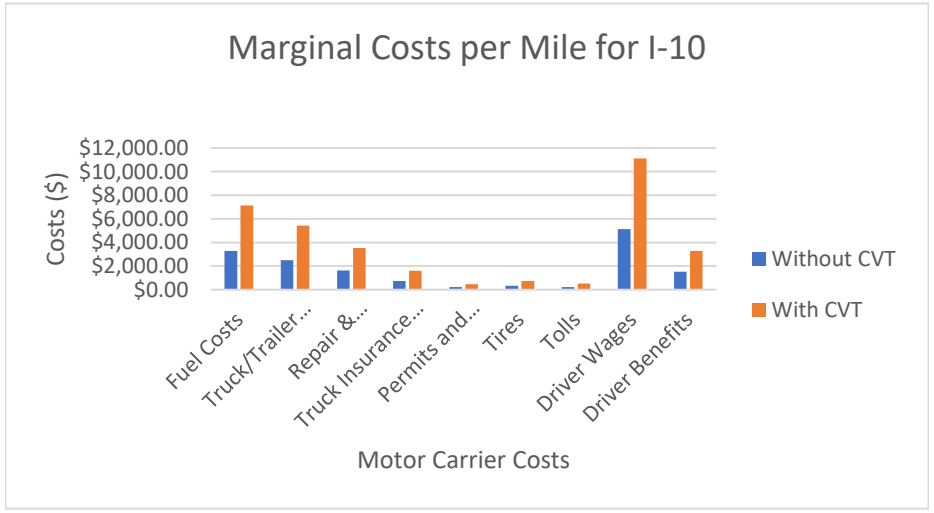

Figure 14: Comparison for marginal motor carrier operational costs for I-10 for the 'without CVT' and the 'with CVT'

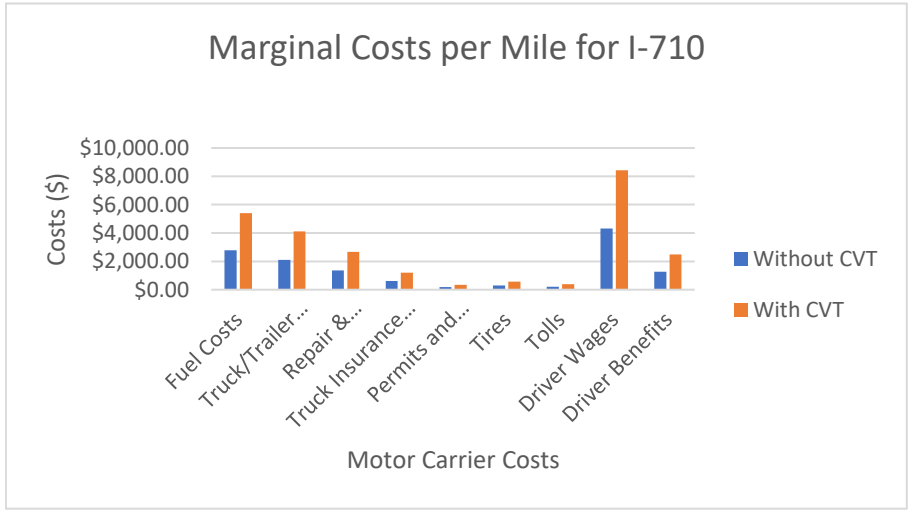

Figure 15: Comparison for marginal motor carrier operational costs for I-710 for the 'without CVT' and the 'with CVT'

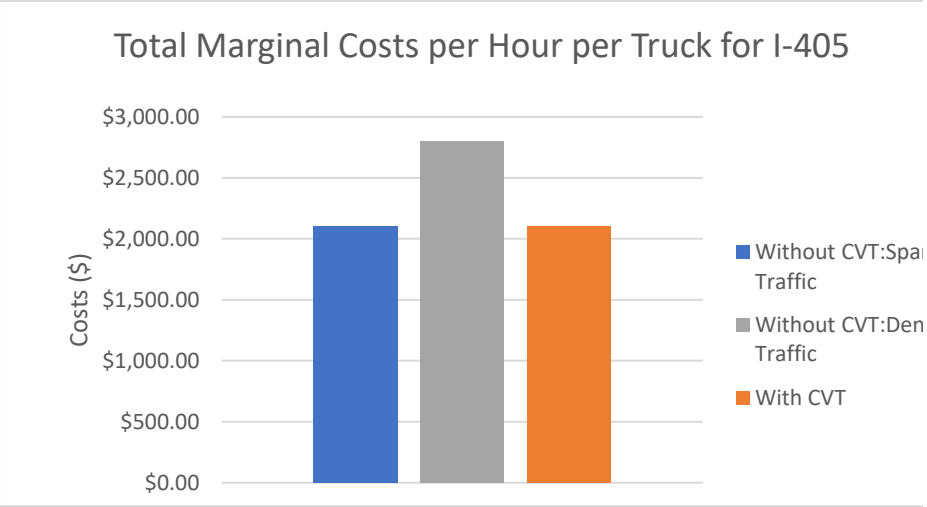

Figure 16: Comparison for total operational costs per hour for I-405 for the 'without CVT' and the 'with CVT'

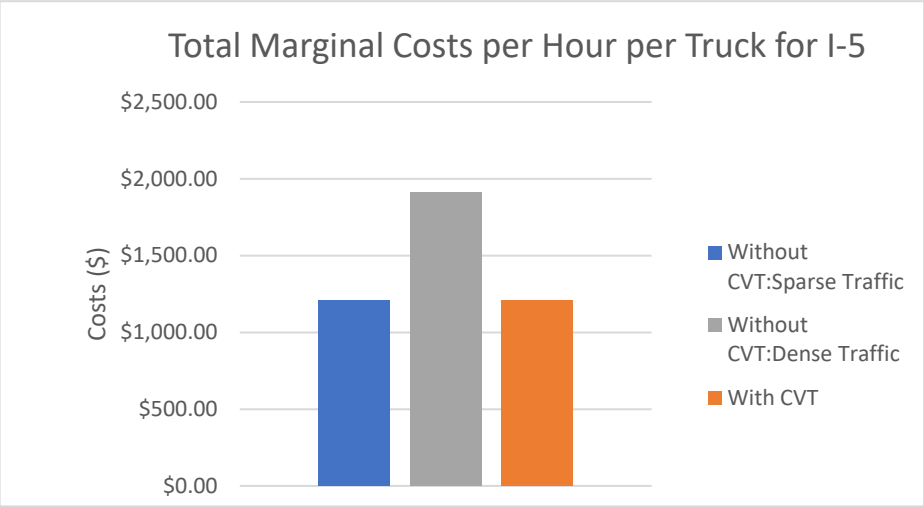

Figure 17: Comparison for total operational costs per hour for I-5 for the 'without CVT' and the 'with CVT'

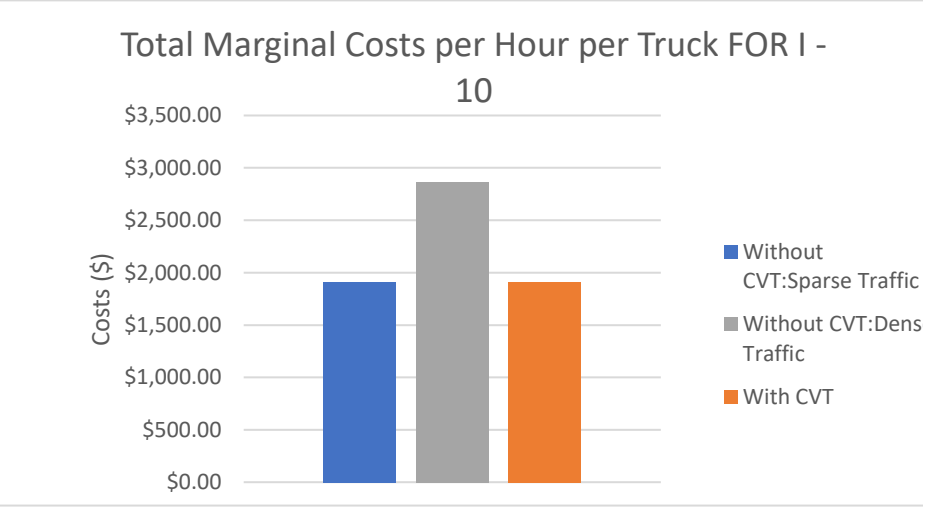

Figure 18: Comparison for total operational costs per hour for I-10 for the 'without CVT' and the 'with CVT'

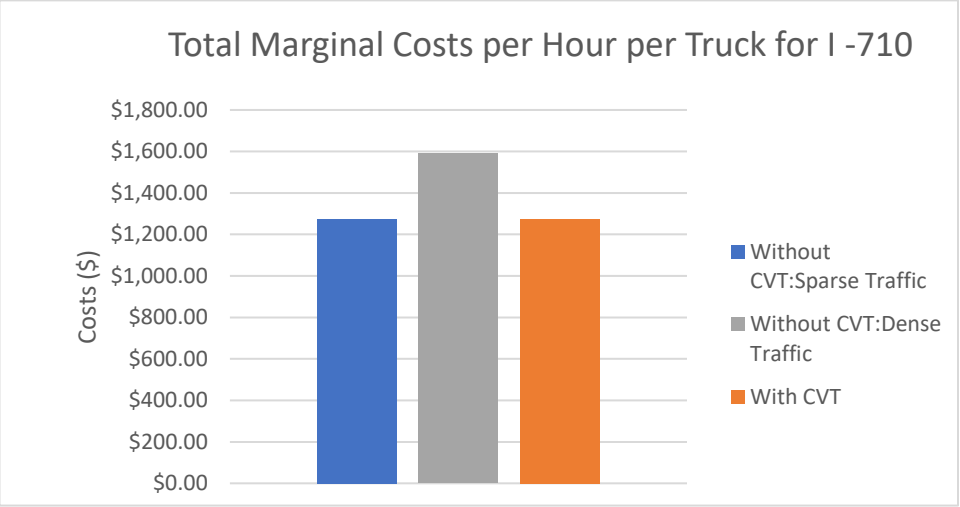

Figure 19: Comparison for total operational costs per hour for I-710 for the 'without CVT' and the 'with CVT'

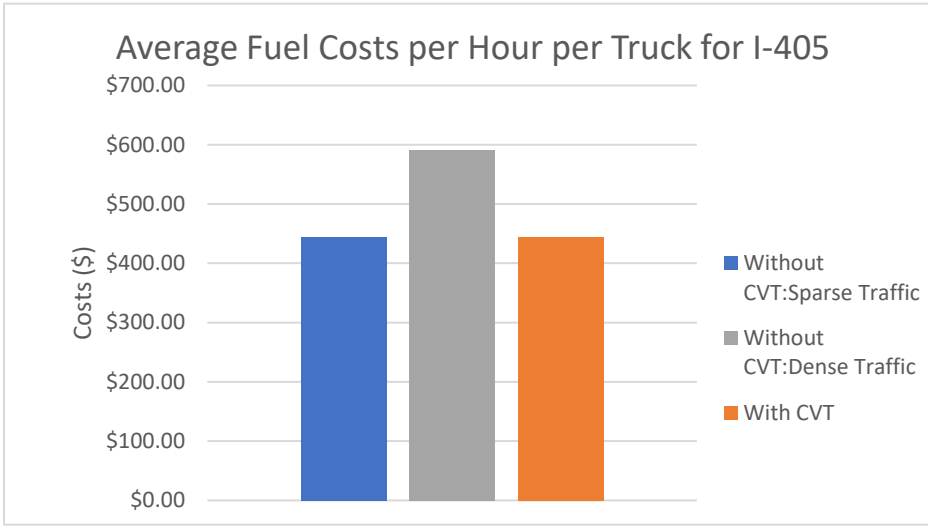

Figure 20: Comparison for fuel operational costs per hour for I-405 for the 'without CVT' and the 'with CVT'

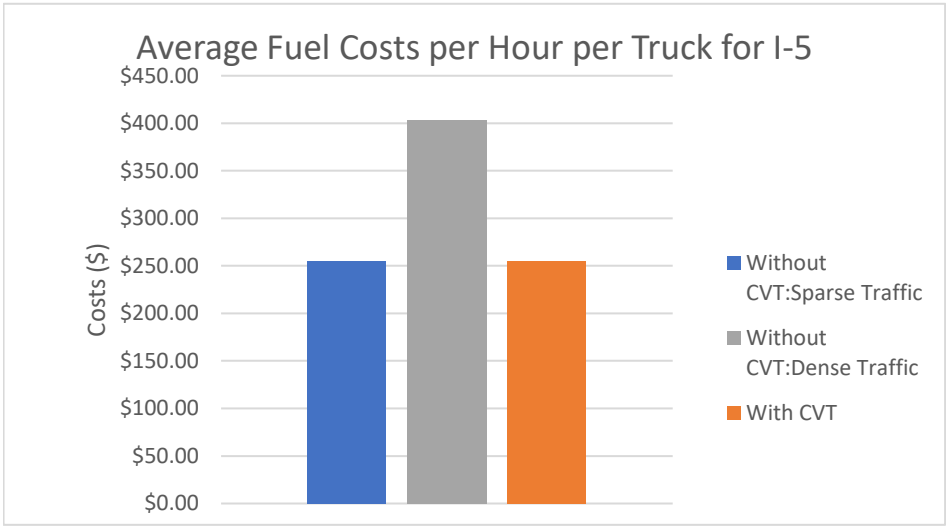

Figure 21: Comparison for fuel operational costs per hour for I-5 for the 'without CVT' and the 'with CVT'

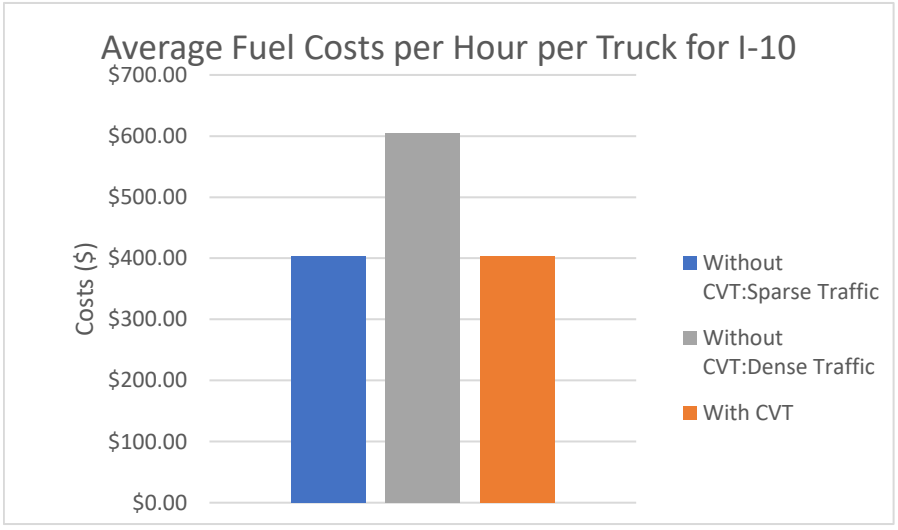

Figure 22: Comparison for fuel operational costs per hour for I-10 for the 'without CVT' and the 'with CVT'

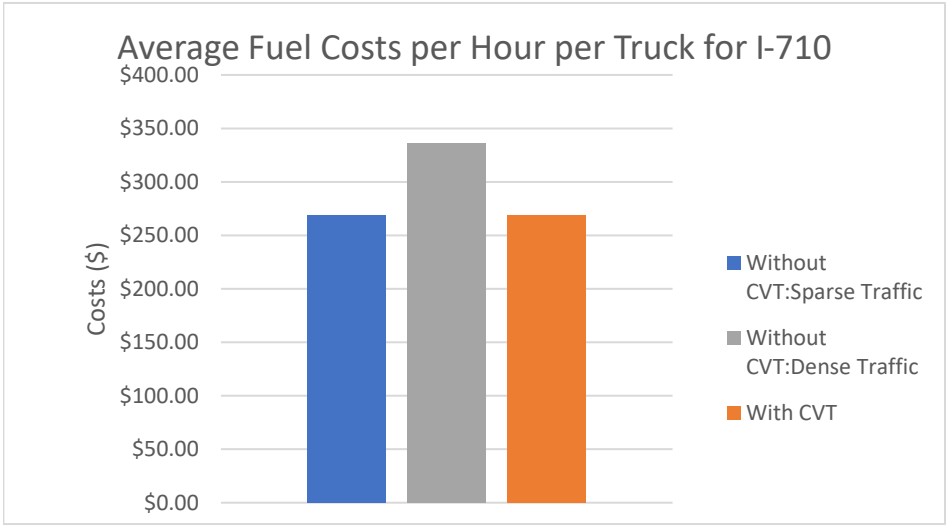

Figure 23: Comparison for fuel operational costs per hour for I-710 for the 'without CVT' and the 'with CVT'

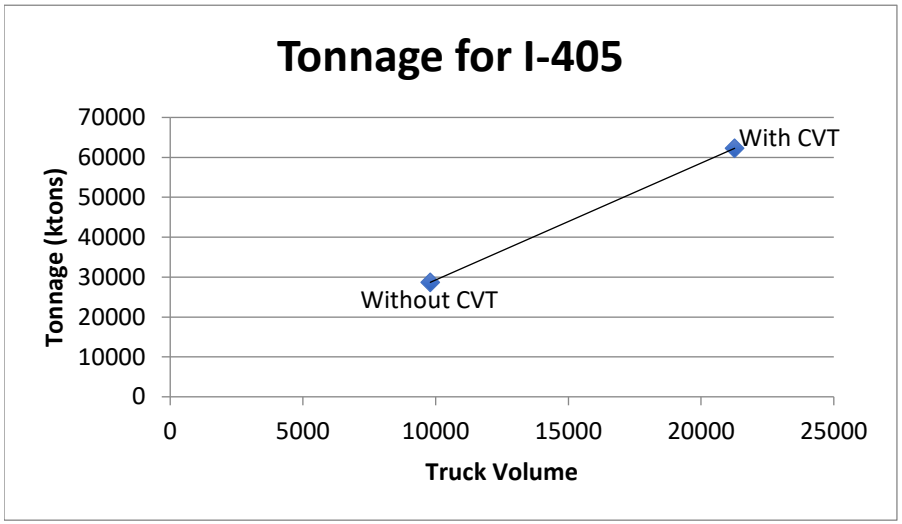

Figure 24: Comparison for total tonnage for I-405 for the 'without CVT' and the 'with CVT'

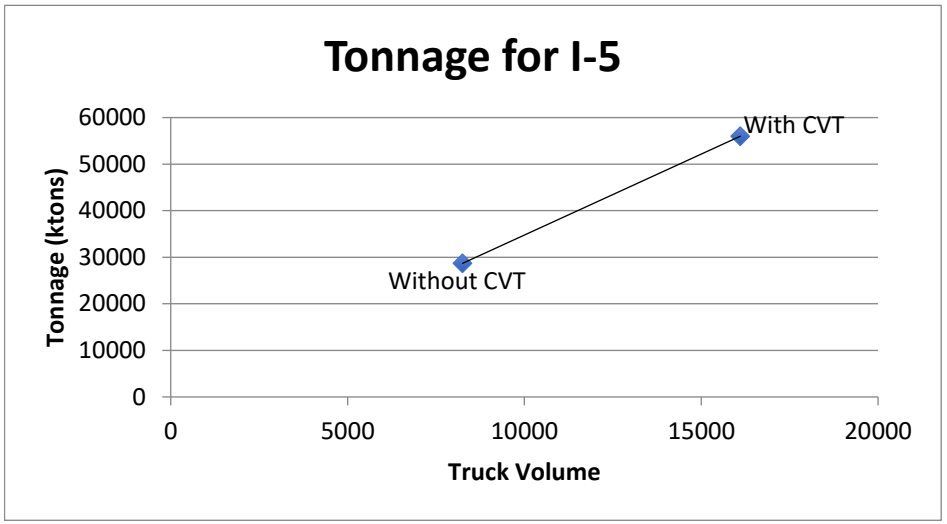

Figure 25: Comparison for total tonnage for I-5 for the 'without CVT' and the 'with CVT'

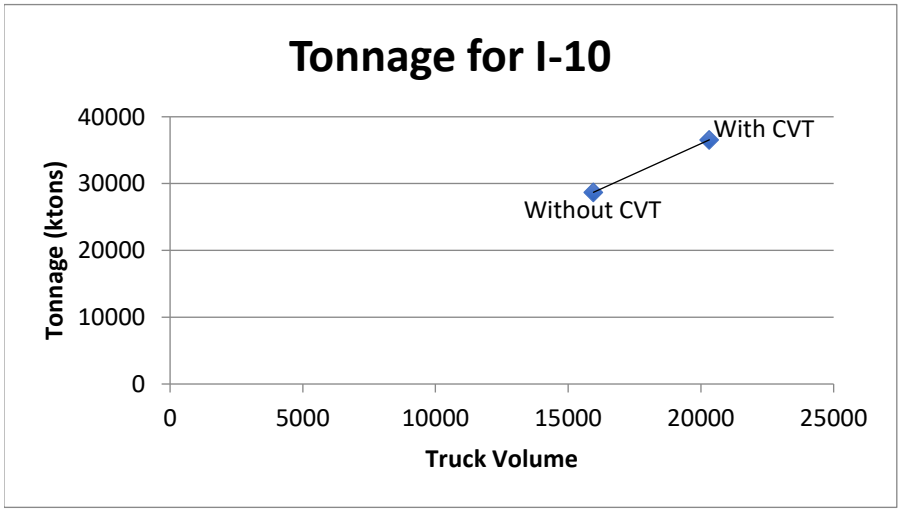

Figure 26: Comparison for total tonnage for I-10 for the 'without CVT' and the 'with CVT'

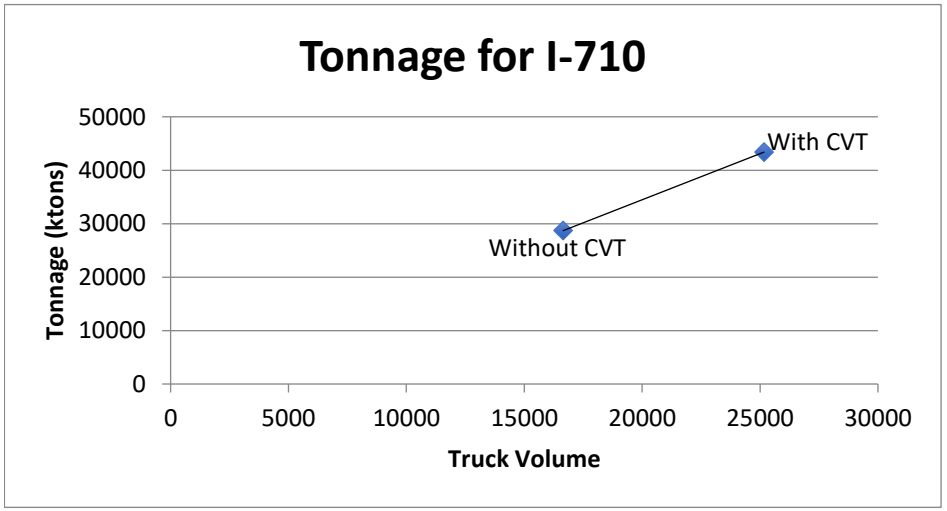

Figure 27: Comparison for total tonnage for I-710 for the 'without CVT' and the 'with CVT'

Concluding Remarks

This research aims to understand the implications of CVT implementation for multimodal freight operations in determining efficient routes for mobility and resilience with connected vehicles' network reliability, and estimating economic costs for CVT-induced route guidance for mobility and resilience. The influence of CVT using vehicle-to-vehicle (V2V) and vehicle-to-infrastructure (V2I) communications on routing of the freight vehicles in the multimodal operations becomes critical for commercial trucks, which, unlike freight rail, have some flexibility in detouring and deviating in order to access other links and nodes of the highway network to complete a trip.

The theoretical indicators for mobility and resilience developed in this research are time-sensitive and vary between 0 and 1. This assists in easy interpretation in the multimodal context. Thus, an indicator value of 0 denotes poor or low mobility/resilience and a value of 1 denotes high mobility/resilience of a route/path being examined. The tonnage values for each of the links constituting the 11 to 15-mile length are obtained from the year 2012 Freight Analysis Framework (FAF) data- which help in estimating parameter values used in the indicators. The parameter value is found to be in the range of 5 to 12 for the routes of I-405, I-5, I-10 and I-710. These interstates connect one or more intermodal terminals and ports in the Southern California Region. It is also noted that for the length of the segments selected for the routes, I-10 appears to the be worst in terms of the mobility indicator, while ranks better than all the routes in terms of the resilience indicator. I-710 appears to be having much better mobility as compared to rest of the routes. This could be due to high truck volumes experience on the interstate resulting in large total tonnage value. Thus, these values of mobility and indicator obtained here can be used in future as elements to design Connected Vehicle Technology or Intelligent Transportation System where rerouting of vehicles will be necessary to produce an efficient freight network.

Findings in this research also indicate that decreasing the value of micro-level reliability, the macro-level reliability will tend to decrease as well. This can be further corroborated with the fact that a low micro-level reliability among individual vehicles of a cluster on an average will lead to low macro-level reliability of the group of clusters.

Further, it is observed that the ratio of theoretical number of vehicles with sensors to total number of vehicles on highway is almost 1 when the optimum radius of transmission range is greater than 1500 feet for traffic densities lower than 9 veh/mile (under sparse traffic conditions).

This optimum radius for transmission range is higher than 55 feet for traffic densities lower than 100 veh/mile with dense traffic conditions. Irrespective of the density of the freight vehicles around an intermodal terminal, port or airport (i.e. congested or uncongested highway with trucks), the expression for the average distance to the closest freight truck does not change. As the length of the highway segment increases, there is linear increase in the average size of connected *k*-component (i.e. *k* trucks). However, there is exponential increase in the average size of the connected *k*-component (trucks) with increase in density of vehicles and/or with increase in sensor transmissions radius. This information is useful in determination of optimum radius of sensor radius when freight vehicles are moving in a platoon.

Cost estimation of routes on I-405, I-5, I-10 and I-710 show that there are savings in fuel costs per hour for the 'with CVT' as compared to the 'without CVT' case. In addition, there is significant increase in total tonnage transported under 'with CVT' case as compared to the 'without CVT' case for all the four routes analyzed.

Acknowledgement

The authors would like to thank METRANS for funding this research.

References

[1] Freight FAST Act Factsheet, U.S. Department of Transportation, accessed on March 20, 2016. https://www.transportation.gov/fastact/freight-factsheet.

[2] Intelligent Transportation System Joint Program Office, United States Department of Transportation, accessed on March 20, 2016. http://www.its.dot.gov/landing/cv.htm

[3] "One California", Caltrans, accessed on March 24, 2016. http://www.dot.ca.gov/research/operations/one_california/docs/DR1_OneCalifornia_Vol_I_Part_I.pdf

[4] The Integrated Truck Program, Intelligent Transportation Systems Joint Program Office, U.S. Department of Transportation, accessed on March 20, 2016. http://www.its.dot.gov/presentations/pdf/Integrated_Truck_Program.pdf

[5] CV Pilot Deployment Program, Intelligent Transportation System Joint Program Office, United States Department of Transportation, accessed on March 20, 2016. http://www.its.dot.gov/pilots/

[6] Bontekoning, Yvonne M., Cathy Macharis, and Jan J. Trip. "Is a new applied transportation research field emerging?—A review of intermodal rail–truck freight transport literature." Transportation Research Part A: Policy and Practice 38.1 (2004): 1-34.

[7] Jones, W. Brad, C. Richard Cassady, and Royce O. Bowden Jr. "Developing a standard definition of intermodal transportation." Transp. LJ 27 (2000): 345.

[8] Wallbaum, H., Krank, S., & Teloh, R. (2010). Prioritizing sustainability criteria in urban planning processes: Methodology application. Journal of urban planning and development, 137(1), 20-28.

[9] PTP, S. B. G. (2009). Performance-based planning: a practitioner's view of transportation planning in the 21st century. Institute of Transportation Engineers. ITE Journal, 79(9), 48.

[10] Wang, Y. G., Zhang, C. B., Cao, Y., & Liu, B. H. (2012). Access for performance of transportation planning and operations: case study in Beijing metropolitan region. Journal of applied research and technology, 10(4), 491-504.

[11] Act, S. T. (2015). Fixing America's Surface Transportation Act. In 114th Congress of the United States of America, January (Vol. 6).

[12] The FAST Act: Freight Provisions, United States Department of Transportation, accessed on August 12, 2017. https://www.transportation.gov/fastact/freight-factsheet

[13] Fowkes, A. S., Firmin, P. E., Tweddle, G., & Whiteing, A. E. (2004). How highly does the freight transport industry value journey time reliability—and for what reasons?. International Journal of Logistics: Research and Applications, 7(1), 33-43.

[14] Vis, I. F., & De Koster, R. (2003). Transshipment of containers at a container terminal: An overview. European journal of operational research, 147(1), 1-16.

[15] Rodrigue, J. P., Comtois, C., & Slack, B. (2009). The geography of transport systems. Routledge.

[16] Vis, I. F., & De Koster, R. (2003). Transshipment of containers at a container terminal: An overview. European journal of operational research, 147(1), 1-16.

[17] "2015 Urban Mobility Scorecard." Urban Mobility Information. Texas A&M Transportation Institute , n.d. Web. 5 May 2017.

[18] Bontekoning, Yvonne M., Cathy Macharis, and Jan J. Trip. "Is a new applied transportation research field emerging?—A review of intermodal rail–truck freight transport literature." Transportation Research Part A: Policy and Practice 38.1 (2004): 1-34.

[19] Jones, W. Brad, C. Richard Cassady, and Royce O. Bowden Jr. "Developing a standard definition of intermodal transportation." Transp. LJ 27 (2000): 345.

[20] Southworth, Frank, and Bruce E. Peterson. "Intermodal and international freight network modeling." Transportation Research Part C: Emerging Technologies 8.1 (2000): 147-166.

[21] TRB, 1998. Policy options for intermodal freight transportation. Transportation Research Board, National Research Council, Washington, DC

[22] Tsamboulas, Dimitrios, and Seraphim Kapros. "Decision-making process in intermodal transportation." Transportation Research Record: Journal of the Transportation Research Board 1707 (2000): 86-93.

[23] Van Duin, Ron, and Hans van Ham. "A three-stage modeling approach for the design and organization of intermodal transportation services." Systems, Man, and Cybernetics, 1998. 1998 IEEE International Conference on. Vol. 4. IEEE, 1998.

[24] Morris, Jennifer M., P. L. Dumble, and M. Ramsay Wigan. "Accessibility indicators for transport planning." Transportation Research Part A: General 13.2 (1979): 91-109.

[25] Arnab Bhattacharya, Sai Anjani Kumar, M.k Tiwari, and S. Talluri. "An Intermodal Freight Transport System for Optimal Supply Chain Logistics." Transportation Research Part C: Emerging Technologies 38 (2014): 73-84. Web.

[26] Arnab Bhattacharya, Sai Anjani Kumar, M.k Tiwari, and S. Talluri. "An Intermodal Freight Transport System for Optimal Supply Chain Logistics." Transportation Research Part C: Emerging Technologies 38 (2014): 73-84. Web.

[27] Hayuth, Yehuda. "Intermodality, concept and practice: Structural changes in the ocean freight transport industry." (1987).

[28] Mahoney, J. H. "Intermodal freight transportation." Transportation Quarterly 40.1 (1986).

[29] Noritake, Michihiko . "Congestion Cost and Pricing of Seaports." Journal of Waterway, Port, Coastal, and Ocean Engineering 111.2 (1985): 354-70.

[30] Hamad, Khaled, and Shinya Kikuchi. "Developing a measure of traffic congestion: fuzzy inference approach." Transportation Research Record: Journal of the Transportation Research Board 1802 (2002): 77-85.

[31] Schrank, D., S. Turner, and T. Lomax. "Estimates of Urban Roadway Congestion in Major Urban Areas." Texas Transportation Institute, USA (1990).

[32] Taylor, M. A. P. "Exploring the nature of urban traffic congestion: concepts, parameters, theories and models." PROCEEDINGS, 16TH ARRB CONFERENCE, 9-13 NOVEMBER 1992, PERTH, WESTERN AUSTRALIA; VOLUME 16, PART 5. 1992.

[33] D'Este, Glen M., Rocco Zito, and Michael AP Taylor. "Using GPS to measure traffic system performance." Computer-Aided Civil and Infrastructure Engineering 14.4 (1999): 255-265.

[34] Cats, Oded, and Erik Jenelius. "Vulnerability analysis of public transport networks: a dynamic approach and case study for Stockholm." The 5th International Symposium on Transportation Network Reliability (INSTR2012), Hong Kong, 18-19 December, 2012. 2012

[35] Appert, M., Chapelon, L., 2013. Measuring Urban Road Network Vulnerability using Graph Theory: The Case of Montpellier's Road Network. Working Paper,
halshs-00841520, Version 1-8.

[36] Reggiani, A., 2013. Network resilience for transport security: some methodological considerations. Transp. Policy 28, 63–68.

[37] Gao, Jianxi, et al. "Robustness of a network formed by n interdependent networks with a one-to-one correspondence of dependent nodes." Physical Review E 85.6 (2012): 066134.

[38] Hughes, J. F., & Healy, K. (2014). Measuring the resilience of transport infrastructure (No. 546).

[39] National Infrastructure Advisory Council, accessed on October 17, 2017. https://www.dhs.gov/national-infrastructure-advisory-council

[40] Golob, Thomas F., and Amelia C. Regan. "Impacts of information technology on personal travel and commercial vehicle operations: research challenges and opportunities." Transportation Research Part C: Emerging Technologies 9.2 (2001): 87-121.

[41] Mattsson, L. G., & Jenelius, E. (2015). Vulnerability and resilience of transport systems–a discussion of recent research. Transportation Research Part A: Policy and Practice, 81, 16-34.

[42] Chen, L., & Miller-Hooks, E. (2012). Resilience: an indicator of recovery capability in intermodal freight transport. Transportation Science, 46(1), 109-123.

[43] Bruneau, M., Chang, S. E., Eguchi, R. T., Lee, G. C., O'Rourke, T. D., Reinhorn, A. M., ... & Von Winterfeldt, D. (2003). A framework to quantitatively assess and enhance the seismic resilience of communities. Earthquake spectra, 19(4), 733-752.

[44] Vadali, S., Chandra, S., Shelton, J., Valdez, A., & Medina, M. (2015). Economic costs of critical infrastructure failure in bi-national regions and implications for resilience building: Evidence from El Paso–Ciudad Juarez. Research in Transportation Business & Management, 16, 15-31.

[45] Tierney, K., and Bruneau, M. (2007). Conceptualizing and measuring resilience: A key to disaster loss reduction. TR news, (250).

[46] Data & Resources, Federal Railroad Administration, United States Department of Transportation, accessed on March 20, 2016. http://www.fra.dot.gov/Page/P0365

[47] Port Surface Transportation Infrastructure Survey, 2015 The State of Freight, accessed on march 20, 2016. http://aapa.files.cms-plus.com/StateofFreight_Report_final.pdf

[48] Lu, Z., Meng, Q., & Gomes, G. (2016). Estimating link travel time functions for heterogeneous traffic flows on freeways. Journal of Advanced Transportation, 50(8), 1683-1698.

[49] Year 2012 FAF tonnage, Freight Analysis Framework data, accessed on July 1, 2017. https://ops.fhwa.dot.gov/freight/freight_analysis/faf/faf4/netwkdbflow/index.htm

[50] Caltrans GIS Data, accessed on August 16, 2017. http://www.dot.ca.gov/hq/tsip/gis/datalibrary/

[51] Flory, P. J. (1941). Thermodynamics of high polymer solutions. The Journal of Chemical Physics, 9, 660.

[52] Sahimi, M. (1994). Applications of percolation theory. CRC.

[53] Liu, J., Upadhyaya, A., German, R. M. (1999). Application of percolation theory in predicting shape distortion during liquid-phase sintering. Metallurgical and Materials Transactions A, 30(8), 2209-2220.

[54] Albert, R., Barabási, A. L. (2002). Statistical mechanics of complex networks. Reviews of modern physics, 74(1), 47.

[55] Meester, R., & Roy, R. (1996). Continuum percolation (Vol. 119). Cambridge University Press.

[56] Talebpour, A., Mahmassani, H. S., & Hamdar, S. H. (2017). Effect of Information Availability on Stability of Traffic Flow: Percolation Theory Approach. Transportation Research Procedia, 23, 81-100.

[57] Li, D., Zhang, Q., Zio, E., Havlin, S., & Kang, R. (2015). Network reliability analysis based on percolation theory. Reliability Engineering & System Safety, 142, 556-562.

[58] Larson, R. C., & Odoni, A. R. (1981). Urban operations research.

[59] Abul-Magd, A. Y. (2007). Modeling highway-traffic headway distributions using superstatistics. Physical Review E, 76(5), 057101.

[60] Truck Lane Use, Caltrans. Accessed on January 2, 2018. http://www.dot.ca.gov/trafficops/trucks/truck-lane-use.html

[61] Chandra, S. (2014). Safety-based path finding in urban areas for older drivers and bicyclists. Transportation research part C: emerging technologies, 48, 143-157.

[62] Hooper, A., & Murray, D. (2017). An Analysis of the Operational Costs of Trucking: 2017 Update.

Appendix

A1: Travel time variation for select interstates from the Southern California Region

Table A1: The travel time data for I-405 segment in Southern California.

			Travel time in minutes												
Distance (miles)	Node Begin	Node End	**6:00 AM**	**7:00 AM**	**8:00 AM**	**9:00 AM**	**10:00 AM**	**11:00 AM**	**12:00 PM**	**1:00 PM**	**2:00 PM**	**3:00 PM**	**4:00 PM**	**5:00 PM**	**6:00 PM**
1.7	4	5	2	2	3	3	2	2	2	2	2	2	3	2	2
1.3	5	7	2	2	2	2	2	2	2	2	2	2	2	2	2
2.2	7	9B	2	3	3	3	3	3	3	3	3	3	3	3	4.5
3.7	9B	12	4	4	4	4	4	4	4	4	4	8.5	13	17	15.5
2.1	12	15	2	2	2	2	2	2	2	2	3	4.5	6	6.5	6.5
1.5	15	16	2	2	2	2	2	2	2	2	2	2	3	3	3
1.5	16	18	2	2	2	2	2	2	2	2	2	2	3	3	3
2.6	18	21B	3	3	3	3	3	3	3	3	3	3	4	4	3
2.1	21B	22	2	3	2	2	2	2	2	2	2	2	3	3	3
0.6	22	23	1	1	1	1	1	1	1	1	1	1	1	1	1
19.3															

Table A2: The travel time data for I-5 segment in Southern California.

			Travel time in minutes												
Distance (miles)	Node Begin	Node End	**6:00 AM**	**7:00 AM**	**8:00 AM**	**9:00 AM**	**10:00 AM**	**11:00 AM**	**12:00 PM**	**1:00 PM**	**2:00 PM**	**3:00 PM**	**4:00 PM**	**5:00 PM**	**6:00 PM**
1.4	105A	106	2	2	2	2	2	2	2	2	3	3	3	4	4
1.3	106	107C	2	2	2	2	2	2	2	2	2	2	2	4	4
0.9	107C	109	1	1	1	1	1	1	1	1	1	1	2	4	4
1.4	109	110	2	2	2	2	2	2	2	2	2	2	3	4.5	3
2	110	112	2	2	2	2	2	2	2	2	2	2	3	3	3
2.5	112	114	3	3	3	3	3	3	3	3	3	3	3	3	3
1.6	114	116	2	2	2	2	2	2	2	2	2	2	2	2	2
2	116	118	2	5.5	4	2	3	4	3	2	3	4.5	5.5	5.5	4.5
2.2	118	120A	3	5	8.5	5	4	4.5	4	3	4	6	6.5	6	4.5
15.3															

Table A3: The travel time data for I-10 segment in Southern California.

						Travel time in minutes									
Distance (miles)	Node Begin	Node End	**6:00 AM**	**7:00 AM**	**8:00 AM**	**9:00 AM**	**10:00 AM**	**11:00 AM**	**12:00 PM**	**1:00 PM**	**2:00 PM**	**3:00 PM**	**4:00 PM**	**5:00 PM**	**6:00 PM**
1.2	19	20A	2	2	2	2	2	2	2	2	2	2	2	4.5	4.5
0.5	20A	21	1	1	1	1	1	1	1	1	1	1	2	2	2
1.6	21	22	2	2	2	2	2	2	2	2	2	4	5.5	5.5	6
1	22	23A	1	1	1	1	1	1	1	2	2	2	2	2	2
0.6	23A	23B	1	1	1	1	1	1	1	1	1	2	2	2	2
0.8	23B	24	1	1	1	1	1	1	1	1	2	2	2	2	2
0.5	24	26A	2	2	3	2	2	2	2	2	3	3	3	3	3
1.7	26A	27	2	2	3	2	2	2	2	2	2	2	2	3	2
1.1	27	28	2	2	2	2	2	2	2	2	2	2	2	2	2
0.9	28	29A	1	1	1	1	1	1	1	1	1	1	2	2	1
1.9	29A	30	2	2	2	2	2	2	2	2	2	3	8	9	8
11.8															

Table A4: The travel time data for I-710 segment in Southern California.

						Travel time in minutes									
Distance (miles)	Node Begin	Node End	**6:00 AM**	**7:00 AM**	**8:00 AM**	**9:00 AM**	**10:00 AM**	**11:00 AM**	**12:00 PM**	**1:00 PM**	**2:00 PM**	**3:00 PM**	**4:00 PM**	**5:00 PM**	**6:00 PM**
1.5	1A	3A	2	2	4	3	2	2	3	2	3	5.5	5	7	2
1.5	3A	4	2	2	3	2	2	2	3	2	3	3	3	3	2
1.8	4	6B	2	2	2	2	2	2	2	2	2	2	3	3	2
0.9	6B	7	1	1	1	1	1	1	1	1	1	1	1	2	2
1.1	7	8B	1	1	2	2	2	2	2	2	2	2	2	3	3
0.9	8B	9	1	1	1	1	1	1	1	1	1	1	2	2	1
0.9	9	10	1	1	1	1	1	1	1	1	1	2	2	2	1
0.9	10	11	1	1	1	1	1	1	1	1	1	1	1	1	1
1.6	11	12	2	11	10	7	2	2	2	2	3	5.5	5.5	4.5	4
11.1															

A2: Derivation of Optimal Mobility and Resilience Indicators

For a fixed time, *t*, and for the freight truck mode, individual segment travel times are assumed to be constant with the set-up shown in Fig.1. Thus, $\tau_{i,t,k} = \left(\frac{d}{V}\right)$ and let T_n $(= \frac{nd}{V})$ denote the time taken by the truck to travel from the beginning of the freeway ramp at A to exit ramp location B, and encompassing *n* ramps. The expected travel time, $E[t]$, from A to B can be expressed as

$$E[t] = \frac{1}{LW}\left(\frac{2LW}{2n-1}\right)\left[\frac{T_n}{(n-1)}\right] + \frac{1}{LW}\left(\frac{2LW}{2n-1}\right)\left[\frac{2T_n}{(n-1)}\right] + \frac{1}{LW}\left(\frac{2LW}{2n-1}\right)\left[\frac{3T_n}{(n-1)}\right]$$

$$+\cdots+\frac{1}{LW}\left(\frac{2LW}{2n-1}\right)\left[\frac{(n-1)T_n}{(n-1)}\right]$$

$$=\left(\frac{2T_n}{2n-1}\right)\left\{\frac{1}{(n-1)}+\frac{2}{(n-1)}+\frac{3}{(n-1)}+\cdots+\frac{n}{(n-1)}\right\}$$

$$=\left(\frac{2T_n}{2n-1}\right)\left\{\frac{n(n+1)}{2(n-1)}\right\}$$

$$=\left(\frac{2nd}{2n-1}\right)\left\{\frac{n(n+1)}{2V(n-1)}\right\}$$

$$=\left(\frac{nd}{2n-1}\right)\left\{\frac{n(n+1)}{V(n-1)}\right\}$$

With n >> 1, $E[t] \approx \left(\frac{nd}{2V}\right)$

The expected travel time, $E[\Delta_n]$, from ramp location A to a spatially average delivery location in zone *n* via ramp located at B is,

$$E[\Delta_n] = E[t] + \left(\frac{W+d}{4v}\right) = \left(\frac{nd}{2V}\right) + \left(\frac{W+d}{4v}\right) \qquad (1)$$

Mobility Optimization

It can be noted from Eq. (1) that as the number of ramps, *n*, on the freeway increases, there is an increase in the average truck travel time across the freight service area. Using the expression in Eq. (1) and with the uniform spatial distribution of tonnage delivery across the area be ρ_1, the mobility expression can be written as:

Mobility = $m_n = \sum_{j=1}^{n-1} \frac{\rho_1 W d}{E[\Delta_n]} = \frac{(n-1)\rho_1 W d}{\left\{\left(\frac{nd}{2V}\right)+\left(\frac{W+d}{4v}\right)\right\}^{\beta}} = \frac{\rho_1 W d}{\left\{\left(\frac{n}{2}\right)h_1 + h_2\right\}^{\beta} \Big/ (n-1)}$ (2)

where, $h_1 = \left(\frac{d}{V}\right)$ and $h_2 = \left(\frac{W+d}{4v}\right)$. The maximum mobility occurs at

$n^* = \frac{\beta}{\beta-1} + \frac{2\left(\frac{W+d}{4d}\right)\Big/\left(\frac{v}{V}\right)}{\beta-1}$. This is derived below.

Assume, $R_2 = \frac{\left\{\left(\frac{n}{2}\right)h_1 + h_2\right\}^{\beta}}{(n-1)}$ in Eq. (2), thus,

$$\frac{dR_2}{dn} = \frac{\frac{\beta h_1}{2}\left\{\left(\frac{n}{2}\right)h_1 + h_2\right\}^{\beta-1}}{(n-1)} - \frac{\left\{\left(\frac{n}{2}\right)h_1 + h_2\right\}^{\beta}}{(n-1)^2} = 0$$

$$n = n^* = \frac{\frac{\beta h_1}{2} + h_2}{\frac{\beta h_1}{2} - \frac{h_1}{2}} = \frac{\beta + \frac{2h_2}{h_1}}{\beta - 1}$$

$$\frac{d^2 R_2}{dn^2} = \frac{\frac{1}{2^{\beta}}\beta(\beta-1)^2 h_1^{\beta}\left\{n + \frac{2h_2}{h_1}\right\}^{\beta-2}}{\left(\frac{2h_2}{h_1}+1\right)}$$

$$n^* = \frac{\beta + 2V\left(\frac{W+d}{4vd}\right)}{\beta-1} = \frac{\beta + 2\left(\frac{W+d}{4d}\right)\Big/\left(\frac{v}{V}\right)}{\beta-1} = \frac{\beta}{\beta-1} + \frac{2\left(\frac{W+d}{4d}\right)\Big/\left(\frac{v}{V}\right)}{\beta-1}$$

Maximum or minimum of R_2 should yield the respective minimum and maximum for m_n.

Thus, using the critical value of $n = n^* = \frac{\beta + 2\left(\frac{W+d}{4d}\right)\Big/\left(\frac{v}{V}\right)}{(\beta-1)}$, R_2 is minimum for any $\beta > 1$. The minimum value of R results in maximum mobility value in Eq. (2). Note that at $\beta = 1$, the expression for $\frac{dR_2}{dN} < 0$ which makes the mobility expression in Eq. (2) a monotonically

increasing function with respect to *n*. This implies that greater the number of exit ramps greater the accessibility at $\beta = 1$.

Resilience Optimization

Similar to the travel time simplification between two ramps in the mobility expression, resilience (r_n) for the entire freeway stretch AB with *n* ramps, can be expressed as,

$$r_n = \sum_{i=1}^{n} \frac{1}{\left(\tau_{i,t,k}\right)^{\beta}} \times \left(\frac{\exp\left(-\alpha\tau_{i,t,k}\right)}{\sum_{i=1}^{n} \exp\left(-\alpha\tau_{i,t,k}\right)} \right) = \frac{1}{\left\{ \left(\frac{nd}{2V}\right) + \left(\frac{W+d}{4v}\right) \right\}^{\beta}} = \frac{1}{\left\{ \left(\frac{n}{2}\right) h_1 + h_2 \right\}^{\beta}}$$

Thus, R_1 increases for any positive *n* implying that the resilience r_n decreases accordingly.